TITLE:

Odorant receptors tuned to isothiocyanates in *Drosophila melanogaster* and their evolutionary expansion in herbivorous relatives

Authors: Teruyuki Matsunaga[1*], Carolina E. Reisenman[2], Benjamin Goldman-Huertas[3], Srivarsha Rajshekar[2], Hiromu C. Suzuki[2], David Tadres[4], Joshua Wong[5], Matthieu Louis[4], Santiago R. Ramírez[6], Noah K. Whiteman[2, 3*]

Affiliations:

[1] Department of Complexity Science and Engineering, Graduate School of Frontier Sciences, The University of Tokyo, Chiba, Japan

[2] Department of Molecular and Cell Biology, University of California Berkeley, Berkeley, CA

[3] Department of Integrative Biology, University of California Berkeley, Berkeley, CA

[4] Department of Molecular, Cellular, and Developmental Biology, University of California Santa Barbara, Santa Barbara, CA

[5] The Biochemistry, Cellular and Molecular Biology Graduate Program, The Johns Hopkins University School of Medicine

[6] Department of Evolution and Ecology, University of California Davis, Davis, CA

[*]Correspondence to: teru.matsu@edu.k.u-tokyo.ac.jp (T.M.) and whiteman@berkeley.edu (N.K.W.)

KEY WORDS:

Drosophila melanogaster, olfaction, isothiocyanate, odorant receptor, Or42a, *Scaptomyza flava,* herbivory, evolution, Brassicales, AlphaFold2

ABSTRACT:

Plants release complex volatile compounds to attract mutualists, deter herbivores, and deceive pollinators. Here, we used herbivorous specialist flies that feed on mustard plants (*Scaptomyza* spp.) and microbe-feeding species (*Drosophila melanogaster* and *Scaptomyza* spp.) to investigate how plant-derived electrophilic toxins such as isothiocyanates (ITCs) affect insects, and how flies detect these

compounds through olfaction. In survival assays, *D. melanogaster* exposed to volatile allyl isothiocyanate (AITC), a toxin derived from many Brassicales plants, were acutely intoxicated, demonstrating the high toxicity of this volatile compound to non-specialized insects. Through single sensillum recordings (SSR) from olfactory organs and behavioral assays, we found that the Odorant receptor 42a (Or42a) is necessary for AITC detection and behavioral aversion. Comparative transcriptome and RNA FISH studies across the drosophilid genus *Scaptomyza* revealed lineage-specific triplication of *Or42a* in the Brassicales specialists and a doubling of *Or42a*-positive-olfactory sensory neurons. Heterologous expression experiments showed that Or42a paralogs in Brassicales-specialists exhibited broadened sensitivity to ITCs in a paralog-specific manner. Finally, AlphaFold2 modeling followed by site-directed mutagenesis and SSR identified two critical amino acid substitutions that conferred *Or42a* heighten sensitivity to Brassicales-derived ITCs. Our findings suggest that ITCs, which are toxic to most insects, can be detected and avoided by non-specialists like *D. melanogaster* through olfaction. In Brassicales specialists, these same Ors experienced gene duplication events that resulted in an expanded sensitivity to ITC compounds. Thus, the insect's olfactory system can rapidly adapt to toxic ecological niches provided by chemically-defended host plants through co-option of chemosensory capabilities already present in their ancestors.

INTRODUCTION:

Plants have evolved the ability to synthesize a diverse array of potentially toxic specialized metabolites that provide resistance against insect herbivory. In turn, herbivorous insects have evolved diverse morphological, physiological, and behavioral counter-strategies to avoid these chemicals if encountered, or to mitigate their effects if ingested (Mithöfer and Boland 2012). Some herbivores even co-opt these plant toxins as oviposition or feeding stimulants and chemical defenses of their own. For example, monarch butterfly (*Danaus plexippus*) larvae evolved target site insensitivity in the sodium potassium ATPase against the cardenolides released from milkweed (*Asclepias* spp.) host plants upon wounding (Dobler et al. 2012). The caterpillars sequester these heart poisons, which serve as effective defenses against predation throughout the life of the insect (Reichstein et al. 1968). Although cardenolides have one major molecular target in insects, some plant toxins are far more promiscuous in their modes of action, which presents a different "evolutionary hurdle" ((Southwood 1972) to herbivores.

For example, to defend themselves against herbivores, Brassicales plants that include mustards (Brassicaeae) have evolved a sophisticated chemical defense system that produces promiscuous electrophilic toxins (Ahuja et al. 2010). These plants produce non-toxic glucosinolates from various amino acid precursors that are hydrolyzed *in planta* to form toxic compounds that include electrophilic isothiocyanates (ITCs) (Hopkins et al. 2009). ITCs are defined by a R−N=C=S functional group wherein the carbon is attacked by nucleophiles such as the sulfhydryl groups of cysteines. For example, allyl isothiocyanate (AITC) is derived from radish [*Raphanus sativus* (Cuellar-Nuñez et al. 2022)], while butyl isothiocyanate (BITC) and other ITCs bearing similar structures are derived from cabbage [*Brassica oleracea* (MacLeod et al. 1989)]. The chemical diversity of glucosinolates allows Brassicales plants to effectively deter a wide array of herbivorous insects because different species have different mixtures of glucosinolates, making it more difficult for insects to adapt (Winde and Wittstock 2011).

One herbivorous insect lineage that has evolved to cope with more promiscuous toxic plant metabolites like ITCs are leaf-mining drosophilid flies in the genus *Scaptomyza* (e.g., *S. flava*) which are specialized primarily on Brassicales plants. *Scaptomyza* species form a clade that is phylogenetically nested within the paraphyletic *Drosophila* subgenus. Gloss et al. (2014) found that yeast-feeding *Drosophila melanogaster* (*D. melanogaster*) uses promiscuous glutathione *S*-transferase (GST) in the gut to detoxify dietary ITCs released from glucosinolate-bearing Brassicales plants like thale cress (*Arabidopsis thaliana*), broccoli (*Brassica oleracea*) and wasabi (*Eutrema japonicum*). Further, they characterized a set of *Scaptomyza*-specific GSTs which experienced rapid gene duplication and non-synonymous changes during the evolution of herbivory that resulted in among the most efficient GSTs known from animals in detoxifying ITCs (Gloss et al. 2014; Gloss et al. 2019). Additionally, Brassicales-feeding *Scaptomyza* flies may minimize their exposure to glucosinolate-derived toxins by selectively ovipositing on leaves that contain lower glucosinolate concentrations (Humphrey et al. 2016).

Insects can behaviorally avoid toxic chemicals through gustation and olfaction (e.g. (Bernays and Chapman 1987; Stensmyr et al. 2012; Scott 2018; Chen and Dahanukar 2020; Dweck and Carlson 2020). In *D. melanogaster*, physical contact of ITCs by the tarsi and proboscis induces behavioral aversion through gustatory receptor cells in those organs that express the nociceptive “wasabi receptor” TrpA1 and Painless (Al-Anzi et al. 2006; Kang et al. 2010; Kim et al. 2010; Mandel et al. 2018). Volatile exposure to extracts containing phenethyl isothiocyanate (PITC) from turnip or rutabaga kills

90 *D. melanogaster*, suggesting that volatile PITC is toxic to these insects, at biologically meaningful
91 concentrations (Lichtenstein et al. 1964). Coupled with more recent findings of how volatile allyl
92 isothiocyanate (AITC) causes aversion in fire ants (*Solenopsis invicta*) (Hashimoto et al. 2019), this
93 intriguing finding raises the possibility that insects have evolved olfactory sensory neurons (OSNs) that
94 detect plant-derived electrophilic compounds such as ITCs, leading to olfactory-mediated behavioral
95 avoidance in generalists, as has been found in the gustatory system.

96 *Scaptomyza* includes species that are both non-herbivorous (e.g., microbe-feeding) and
97 herbivorous species (Aguilar et al. 2024). However, the most recent common ancestor of the herbivores
98 is hypothesized to have been microbe-feeding based on ancestral state reconstruction (Whiteman et al.
99 2011; Whiteman et al. 2012; Peláez et al. 2023). Of particular interest are the Brassicales plant
100 specialists *S. flava* and *S. montana*, which are closely related species in the exclusively herbivorous
101 subgenus *Scaptomyza* of the genus *Scaptomyza* (Kim et al. 2021). Additionally, *Or85d, Or42b, Or9a*
102 and *Or22a,* which in *D. melanogaster* mediate the olfactory detection of fermentation products of
103 brewer's yeast and other microbes, have been lost in a stepwise fashion during the evolution of the
104 herbivory in *Scaptomyza* (Goldman-Huertas et al. 2015). Furthermore, the *S. flava* paralogs of the
105 antennal odorant receptor Or67b, which in *D. melanogaster* is present as a single copy and responds to
106 green leaf volatiles such as *trans*-3-hexenol, respond in *S. flava* to a subset of ITCs (Matsunaga et al.
107 2021). Although there has been some progress, whether and to what extent generalist insects avoid
108 volatile electrophilic compounds like ITCs on the one hand, and how evolution has reshaped the sensory
109 receptors of specialists to facilitate both aversion and attraction on the other, is still largely unknown, yet
110 is a central problem in understanding how organisms invade toxic niches.

111 We addressed this question in *D. melanogaster* and a set of *Scaptomyza* spp. exhibiting a
112 gradient in microbe-feeding and plant-feeding habits. We first recapitulated the experiments of
113 Lichtenstein et al. (1964), but instead of PITC, we used the more widely used AITC and found that *D.*
114 *melanogaster* is rapidly killed by exposure to moderate concentrations of volatile AITC, demonstrating
115 the insecticide potency of this electrophilic compound. This indicated that *D. melanogaster* may have
116 evolved odorant receptors that respond to and release aversive behaviors toward volatile ITCs. We
117 found that Or42a, which is expressed in maxillary palp-specific pb1a OSNs, is highly sensitive to AITC
118 and is necessary for behavioral aversion to this compound in *D. melanogaster*. Furthermore, we
119 discovered that mustard plant specialist *Scaptomyza* fly species *S. flava* and *S. montana*, but not

120 microbe-feeding *Scaptomyza* species, have expanded their ITC sensitivity range. This was coupled with
121 a concomitant increase in the number of *Or42a*-positive-OSNs in *S. flava* and *S. montana*, and with a
122 triplication of the *Or42a* gene in *S. flava*. We then used site directed mutagenesis and found that via just
123 two amino acid substitutions, one of these Or42a paralogs in *S. flava* switched its sensitivity from odors
124 that activate the Or42a of microbe feeders to odors that activate mustard specialists, paralleling the niche
125 shift of the mustard-feeding *Scaptomyza*. Taken together, these results illustrate how plant-derived
126 volatile toxins like electrophilic ITCs can negatively impact insect behavior and fitness, how the insect
127 olfactory system detects them leading to behavioral avoidance, and how host-plant specialization
128 reshapes the organization and molecular function of toxin-detecting Ors.

129

130 **MATERIAL AND METHODS:**

131 **Fly Husbandry**

132 Microbe-feeding *D. melanogaster* was reared on cornmeal medium. Microbe-feeding *S. pallida*
133 (subgenus *Parascaptomyza*) and *S. hsui* (subgenus *Hemiscaptomyza*) were reared in vials of cornmeal
134 molasses media covered with a mixture of Carolina biological supply instant *Drosophila* media
135 (Burlington, NC) mixed with blended spinach leaves, and then covered with a layer of defrosted frozen
136 spinach leaves. The obligate leaf-miners *S. flava* and *S. montana* (subgenus *Scaptomyza*) were cultivated
137 on potted fresh laboratory-grown *Arabidopsis thaliana* Col-0. Isofemale lines of microbe feeding *S. hsui*
138 and *S. pallida*, as well as the herbivorous *S. montana,* were collected along Strawberry Creek on the UC
139 Berkeley Campus in Berkeley, California, USA (Kim et al. 2021), and a line of *S. flava* was collected in
140 from a meadow near Dover, New Hampshire, USA. All species were kept at 23±2°C and 60% relative
141 humidity in a 10L:14D light cycle under fluorescent ballast lights. The following lines (stock #) were
142 obtained from the Bloomington *Drosophila* Stock Center: *Orco* (23130), *Or42a-/-* (60821), *Or42a-Gal4*
143 (9970), w^{1118} (3605), $TrpA1^{1}$ (26504), and a genetic background control for the $Or42a^{-}$ line (68384). The
144 $Or67d^{Gal4}$ line was a gift from the laboratory of Barry J. Dickson.

145

146 **Single sensillum recordings (SSRs)**

147 One to five day-old fed female flies were prepared for Single Sensillum Recording (SSR) as
148 described in (Matsunaga et al. 2021). Briefly, a silicon tube delivering a constant flow of charcoal-

149 filtered air (16 ml/min, measured using a flowmeter, Gilmont Instruments, USA) was placed near the
150 fly's head capsule, and the tip of the stimulation pipette (50 ml) was inserted into the constant air stream.
151 The stimulation pipette contained a 0.5 cm x 5 cm piece of filter paper loaded with 20 µl of an odorant
152 solution or the solvent control. A pulse of clean air (duration = 1 sec) was delivered to the stimulus
153 pipette using a membrane pump operated by a Stimulus Controller CS 55 (Syntech, Buchenbach,
154 Germany). Sensilla identification was conducted by using the following diagnostic odorants (as
155 described in (Dweck et al. 2016; Gonzalez et al. 2016); all >95% pure, Sigma-Aldrich, St. Louis, MO,
156 USA): ethyl acetate (CAS # 141-78-6) for identifying *D. melanogaster* (*Dmel*) pb1a; AITC (CAS # 57-
157 06-7) for identifying *Scaptomyza* pb1a-like olfactory sensory neurons (OSNs); 4-ethylguaiacol (CAS#
158 2785-89-9) for identifying *Dmel* and *Scaptomyza* pb1b-like OSNs; fenchone (CAS# 1195-79-5) for
159 identifying *Dmel* and *Scaptomyza* pb2a OSNs; guaiacol (CAS# 90-05-1) for identifying *Dmel* and
160 *Scaptomyza* pb2b OSNs; phenethyl acetate (CAS# 103-45-7) for identifying *Dmel* pb3b, *Sfla* pb3b, and
161 *Smon* pb3a-like OSNs; and 2-heptanone for identifying *Shsu* and *Spal* pb3a-like OSNs. All odorants
162 were diluted in mineral oil (CAS 8042-47-5) except γ -hexalactone (CAS # 695-06-7), which was
163 diluted in dimethyl sulfoxide (DMSO: CAS# 67-68-5). Odorants were diluted to 1/100 vol/vol for
164 stimulation unless otherwise noted. Supplementary file 1 lists all the chemicals used in this study.

165 The "net number of spikes/second" was obtained by counting the number of spikes originating
166 from the OSN of interest within a 0.5-second timeframe which started 0.2 seconds after the onset of
167 stimulation. This count was then adjusted by subtracting the background spiking activity (# of spikes
168 within a 0.5 second interval preceding the stimulation), and then doubled to represent the number of
169 spikes/second. In all figures, unless otherwise stated, we represent the "control-subtracted net # of
170 spikes/sec" to odorant stimulation, calculated by subtracting the average net # of spikes/sec in response
171 to the solvent control (mineral oil or DMSO) from the net # of spikes/sec evoked by each odorant
172 stimulation. The BITC to γ-hexalactone spike ratio (Figure 4F and Figure supplement 10) was calculated
173 as: [net # of spikes/sec evoked by BITC/ (net # of spikes/sec evoked by BITC + net # of spikes/sec
174 evoked by γ-hexalactone)]. We used this denominator for the ratio because the control-subtracted net #
175 of spikes by γ-hexalactone occasionally produced negative values (likely a response to the solvent
176 control).

177 The *Or67d*^{GAL4} line was used to generate flies expressing *Or42a* homologs in the at1 "empty
178 neuron" system, as described in (Kurtovic et al. 2007).

179

180 **Survival assay**

181 To investigate the survival of wild-type *D. melanogaster* (Canton-S strain) flies in presence of
182 AITC volatiles, we used a 9 cm diameter plastic petri dish (Nunc, Denmark) with a piece of fabric mesh
183 placed horizontally between the base and the lid, which created two chambers (Figure supplement 1A).
184 The upper chamber housed 8-10 three to five days old male flies, and the lower chamber contained four
185 5 µl drops of the odor solution (or the solvent control) evenly dispersed. Because the mesh prevented the
186 flies from reaching the bottom chamber, insects were exposed to the volatile chemicals but could not
187 directly contact (i.e. taste) the odor solution unless the molecules adhered to the walls of the chamber
188 after volatilizing. After each test started, we counted the number of flies alive every 10 minutes up to
189 one hour and calculated the percentage of survival. Flies exhibiting no movement for >30 seconds were
190 considered dead. AITC or γ-hexalactone were diluted in either mineral oil or DMSO at various
191 concentrations. Survival data analysis was performed using the log-rank (Mantel-Cox) test (Mantel
192 1966).

193

194 **Consumption assay**

195 Groups of 2-4 days old mated female flies (n=11-15) were wet-starved for 24 hours, and then
196 transferred to a vial containing a piece of filter paper (2.7 cm diameter, Whatman, cat. No 1001 125)
197 impregnated with 160 µl of 50 mM D-glucose (Sigma-Aldrich, USA) dyed blue with Erioglaucine (0.25
198 mg/ml, Sigma-Aldrich, St. Louis, MO, USA) (Reisenman and Scott 2019) (Figure supplement 1B). Flies
199 were allowed to feed for 15 minutes (10 minutes in tests with γ-hexalactone), vials were frozen (>60
200 minutes), and the amount of blue dye in the flies' abdomen was scored blind to treatment (see below).
201 The odor source consisted of a strip of filter paper (0.25 cm wide x 1.5 cm long) impregnated with either
202 10 µl of an odorant solution (test) or 10 µl of the solvent (control), which was placed inside a container
203 (1.3 cm long x 0.75 cm diameter) with a meshed bottom affixed to the vial's flug (Figure supplement
204 1B). This allowed diffusion of odors into the fly vial but prevented flies from contacting the odor source.
205 Control tests, with vials containing food solution but only the solvent control inside the meshed
206 container, were conducted in parallel with experimental tests to control for fly cohort and day-to-day
207 variability.

208 Food consumption was estimated by scoring individual flies in each vial blind to treatment using
209 the following five-point scale (Reisenman and Scott 2019): 0 (no dye = no food), 0.25 ("trace" of blue

210 dye), 0.5 (up to ¼ of the abdomen dyed blue), 1 (more than ¼ but less than ½ of the abdomen dyed
211 blue), and 2 (more than ½ of the abdomen dyed blue). For each vial, a single feeding score value was
212 calculated as: $[(0 \times n_0 + 0.25 \times n_{0.25} + 0.5 \times n_{0.5} + 1 \times n_1 + 2 \times n_2) / N]$, where $n_{(0\text{-}2)}$ denotes the number of
213 flies in each score category, and N the total number of flies/vial. Each odor vial datapoint was
214 normalized by dividing the feeding score in presence of odor by the averaged feeding score for the
215 corresponding day and genotype in absence of odor. Normalized data for each genotype and odor was
216 compared against the expected median=1 using one sample signed rank tests. That is, medians
217 significantly less than 1 or more than 1 respectively indicate feeding aversion and enhancement;
218 medians not different from 1 indicate that the odorant did not reduce neither enhanced consumption.
219 Normalized data from control and mutant flies were compared using Mann-Whitney U tests. In all cases
220 results were considered statistically significant if $p<0.05$. The consumption assay data is compiled in
221 Supplementary file 4.
222

223 **Positional olfactory assay**

224 To study the olfactory orientation of insects towards odors, we conducted group assays with fed
225 3-4 days old, mated females (Figure supplement 1C). Flies (n=10-12/test) were briefly anesthetized on
226 ice and placed in a small piece of clear Tygon tube, capped in both sides with the bottom of a conical
227 PCR plastic Eppendorf. After another about 3-4 minutes, the Tygon tube with the anesthetized flies was
228 uncapped and connected to the cut ends of two glass Pasteur pipettes and the assay started; flies usually
229 resume activity after about three-four minutes. Each of the two opposite ends of the pipettes were
230 respectively connected (via a small piece of Tygon tube) to a glass vial (capacity: 0.5 ml) containing 10
231 µl of the odor solution (AITC 1: 500 vol/vol, or γ-hexalactone 1:100 or 1:10 vol/vol) or 10 µl of the
232 control solvent (mineral oil, or DMSO). Tests with apple cider vinegar used 30 µl instead, and water
233 was used as a control. The distal ends of the pipettes were separated from the glass vials with a small
234 piece of fabric mesh, which allowed the odorant to diffuse into the pipette while also preventing insects
235 from contacting the odor source (Figure supplement 1C). The odor and control sides were switched
236 between assays. Assays were conducted on a white surface under white light at 22-24 °C, about 2-6
237 hours after lights on. Once each assay started, the number of flies in the pipette closest to the vial with
238 the odor (referred to as "odor side" or "odorous tube" for simplicity), in the pipette closest to the vial
239 with the solvent control ("control" side/tube), and in the Tygon tube that connected both pipettes
240 (release site) were counted every five minutes until minute 35, and then again at 65 minutes in the case

241 of tests with AITC. For each assay, we calculated the % of insects that made a choice for one or the
242 other tube as: [(#of insects in the odor side + # of insects in the control side) / total number of insects
243 released)] x 100. The percentage of insects that choose the odorous tube was calculated based on the
244 total number of insects that made a choice as: [# of insects in the odor side / (# of insects in the odor side
245 + # of insects in the control side)] x 100. Assays in which less than 40% of insects made a choice for
246 either side at all time points were discarded (<5% of assays). For each fly genotype and odorant, the %
247 of insects that choose the odor side at each time point was compared against the median value expected
248 under the hypothesis that insects distributed at random between the two tubes (50% of insects in each
249 tube) using one-sample signed rank tests. Thus, the insects either avoid the odorous tube (if
250 median<50%) or prefer it (if median>50%). Also, at each time point and for each odor (and
251 concentration when applicable), the responses of *Or42a-/-* and its genetic background control
252 (Bloomington Stock Center # 68384) were compared via Mann-Whitney U tests. In all cases results
253 were considered significant if $p<0.05$. The positional olfactory assay data is included in Supplementary
254 file 5.
255

256 **RNA-sequencing of maxillary palps**

257 Newly emerged adults of *S. flava* and *S. pallida* were collected from our colony and kept in
258 humidified vials with 10% honey water until dissection, to minimize potential differences in nutrition
259 resulting from differences in the two species' larval diet. Three to ten days old flies were anesthetized
260 with CO_2, and their maxillary palps were hand-dissected using forceps. Approximately 100-120 flies
261 were pooled for a single sample. The dissected tissues were directly collected in LB+TGA lysis buffer
262 from Reliaprep RNA Tissue Miniprep System (Promega, USA), and homogenized using a Biomasher
263 Standard homogenizer (Takara Bio Inc., USA) in a dry ice ethanol bath. The sample lysates were stored
264 at -80°C until RNA extraction. Total RNAs were extracted from the lysates using ReliaPrep RNA Tissue
265 Miniprep System (Promega, USA) according to the manufacturer's protocol, and quantified using a
266 Qubit RNA High Sensitivity kit (Thermo Fisher Scientific, USA). Library preparation was performed at
267 the Functional Genomics Laboratory (FGL) at UC Berkeley. Due to the low yields of our maxillary
268 palp-derived total RNAs, cDNA libraries were first produced by Takara SMART-Seq mRNA Ultra-low
269 input RNA kit (Takara Bio Inc., USA) with 8 cycles of PCR for the amplification, and then processed by
270 KAPA HyperPrep kit for DNA (Roche Sequencing, USA) with 9 cycles of PCR for attaching in-house
271 sequencing adapters and index primers. cDNA libraries were then transferred to the Vincent J. Coates

272 Genomics Sequencing Laboratory (GSL) at UC Berkeley and sequenced on an Illumina NovaSeq 6000
273 150 PE S4 flowcell, targeting 25M read pairs per library. For read mapping, we used previously reported
274 reference genome assemblies and gene annotations from *S. flava* (Peláez et al. 2023) and *S. pallida* (Kim
275 et al. 2021) for subsequent bioinformatic analyses. Raw RNA-seq reads were filtered using Fastp
276 v0.21.0 (Chen et al. 2018) and mapped to the respective reference genomes using STAR v2.7.1a (Dobin
277 et al. 2013) to generate multiple alignment (BAM) files, which were then converted to read count data
278 using HTseq v0.9.1 (Anders et al. 2015). Count data for the Or gene family were converted to RPM
279 (reads per million); data is compiled in Supplementary file 6.
280

281 **HCR RNA FISH**

282 One-to-four-day-old female *S. flava* and *S. pallida* were collected and anesthetized with CO_2.
283 Whole mouthparts were removed proximal to the attachment of the maxillary palps with Inox 5 forceps
284 (Fine Science Tools, Foster City, CA) on a Sylgard-covered petri dish. Mouthparts from each species were
285 immediately placed in 2 mL of fixative (4% vol/vol paraformaldehyde in 1x phosphate buffered saline
286 with 3% vol/vol Triton X-100 added, PBST) in a LoBind Eppendorf tube, and fixed for 22 hours at 4°C
287 on a nutator.

288 Fixative was carefully pipetted out from samples and replaced with 2 mL of cold (4°C) 3% PBST,
289 and tubes were agitated on a nutator for 5 minutes. This step was repeated once more and then again with
290 cold 0.1% PBST; samples were then washed with 1 mL of cold 0.1% PBST 4 times and agitated on a
291 nutator (5 min for each wash). PBST was removed and replaced with 300 µL of warm (37°C) HCR RNA
292 FISH probe hybridization buffer (Molecular Instruments, Inc., Los Angeles, CA) and incubated for 30
293 minutes. The probe hybridization solution was prepared by adding 5µL of 1µM of probe B1-*Spal Or42a*
294 and probe B2-*Spal Orco* (or probe B1-*Sfla Or42a* and probe B2-*Sfla Orco*) to 300 µL of pre-heated probe
295 hybridization buffer for the *S. pallida* or the *S. flava* tissues and kept at 37°C. Finally, the buffer was
296 replaced with the preincubated probes in hybridization buffer and kept at 37°C for 22 hours.

297 Samples were next washed 3 times with 500 µL of preheated (37°C) probe wash buffer for 5 min
298 on a heating block. Ten µL of 3µM amplification hairpins one and two of b1-488 and b2-637 HCR
299 amplifiers (Molecular Instruments, Inc., Los Angeles, CA) were snap cooled on a thermocycler at 95°C
300 for 90 secs and then at 20°C for 30 min, and then covered with aluminum foil. Samples were washed 3
301 times with 500 µL of 0.75M NaCl, 75mM sodium citrate and 0.1% Tween-20 vol/vol (SSCT) at room
302 temperature for 5 minutes, and then incubated in 500 µL amplification buffer (Molecular Instruments,

303 Inc., Los Angeles, CA) for 30 minutes at room temperature. Snap cooled hairpins were added to two vials
304 containing 300 µL of amplification buffer for each species. The amplification buffer was removed from
305 the samples and replaced with the hairpin solution; tubes were covered in aluminum foil and incubated at
306 room temperature for 22 hours.

307 Samples were washed twice with 500 µL of SSCT solution for 5 minutes, twice for 30 minutes,
308 and finally washed again for 5 minutes (vials were kept on a nutator in between washes). Samples were
309 then stained with 300 nM DAPI stain in 0.1% PBST for 15 minutes, and then washed 3 times with 0.1%
310 PBST for 5 minutes. Tissues were transferred to a microscope slide and mounted in a drop of ProLong
311 diamond antifade mounting (Life Technologies Corp., Eugene, OR) and stored at 4°C until examination.
312 Confocal imaging of fixed samples was performed using a Zeiss LSM 880 microscope in the AiryScan
313 mode. Raw images were processed using Zeiss ZEN Black software. *Orco*-positive cells (visualized with
314 the 488 nm laser) and *Or42a*-positive cells (visualized with the 633 nm laser) were manually counted
315 using the "Cell Counter" plugin in Fiji (ImageJ) software. Supplementary file 7 contains cell counts of
316 RNA FISH.

317

318 ***Scaptomyza Or42a* gene cloning and generation of *UAS* lines**

319 RNA was isolated from 15-25 days laboratory-reared adults of both sexes of *S. pallida* and *S. flava*
320 using the ReliaPrep Miniprep system (Promega, W.I., USA). Complementary DNA (cDNA) was
321 synthesized using the qScript cDNA Supermix (Quantabio, Beverly, MA, USA). The paralogs were
322 amplified via touchdown PCR, using primers that target the highly variable regions of the 5' and 3'
323 untranslated regions (UTRs). The single *Or42a* gene of *S. pallida* was amplified using touchdown PCR
324 with primers targeting the coding region (Q5 DNA Polymerase, #M0491, NEB) (Supplementary file 8).
325 All PCR products underwent gel purification (11-300C, Zymo Research) and were subsequently cloned
326 using the Gibson Assembly (E2611S, NEB) following the manufacturer's instructions into the UAST-
327 attB vector [DGRC Stock 1419; RRID:DGRC1419, (Bischof et al. 2007)]. The ligation products were
328 transformed into DH5α competent cells (T3007, Zymo Research). After confirming the sequences, the
329 5' and 3' UTRs of the plasmids containing the *S. flava Or42a* paralogs were removed. This was
330 achieved by first amplifying the coding region using PCR, followed by gel purification and ligation back
331 into UAST-attB vector via Gibson Assembly. The resultant plasmids were sequence-verified. Finally,
332 these plasmids were microinjected into the attP40 site (P{nos-phiC31\int.NLS}X, P{CaryP}attP40, line

333 # 25709, Rainbowgene) to create transgenic lines for *Spal Or42a*, *Sfla Or42a2*, *Sfla Or42a3* and *Sfla*
334 *Or42a4*. All lines were confirmed by sequencing prior to experiments.

335 **Screen of candidate amino acids using branch-site test and Colabfold 3D prediction**

336 CDS of *Sfla Or42a3* and *Sfla Or42a4* were confirmed by palp RNAseq data using IGV_2.16.0.
337 CDSs of *Sfla Or42a3* and *Sfla Or42a4* were then used as inputs into ColabFold (Jumper et al. 2021;
338 Mirdita et al. 2022). Then the output models ranked first (rank1) were selected, visualized, and 3D-
339 aligned by using PyMol2.5.3. Since previous studies suggested that the binding pockets of odorant
340 receptors are located in the transmembrane region (Butterwick et al. 2018; Del Mármol et al. 2021; Zhao
341 et al. 2024), in silico substitutions of amino acids were individually conducted on *Sfla Or42a3*. The
342 resulting amino acid sequences were then re-inputted into ColabFold, the model with rank1 was
343 selected, and the sequences were 3D-aligned with *Sfla* Or42a4. This process was repeated until the 3D
344 structures of transmembrane regions between the chimera and *Sfla* Or42a4 matched in PyMol space. All
345 pdb files used in this study are included in Supplementary file 9.

346

347 **Site-directed mutagenesis**

348 Conventional PCR was conducted using plasmids of *Sfla Or42a3* as backbone (Q5 DNA
349 polymerase, #M0491, NEB; Supplemental File 1). Primers were designed to introduce the point
350 mutations (Supplementary File 1). The PCR product underwent gel purification (11-300C, Zymo
351 Research) and the methylated plasmids were digested with DpnI for 1 hour at 37°C (QuickChange,
352 Agilient Technology, USA). Ligation was performed by incubation at 16°C for 30 minutes (DNA
353 ligation kit Mighty mix, Takara, Japan) and the products were transformed into DH5α competent cells
354 (Takara, Japan). After confirming the sequence, the plasmid was microinjected into the attP40 site
355 (P{nos-phiC31\int.NLS}X, P{CaryP}attP40, line # 25709, Rainbowgene) to create transgenic A181D
356 S307P fly. The line was confirmed by sequencing prior to experiments.

357

358 **RESULTS**

359 **Volatile AITC rapidly kills *D. melanogaster*.**

360 We conducted survival assays with various concentrations of volatile AITC (from 1/500 to 1/2.5
361 vol/vol). In our experimental setup, a fabric mesh separated the chamber containing the flies from the

362 chamber containing one of the ITC solutions (Figure supplement 1A) and therefore, flies were exposed
363 to volatile AITC but could not contact (i.e. taste) the AITC solution directly. While all animals in both
364 the control treatment and those exposed to AITC 1:250 and 1:500 vol/vol survived, most flies exposed
365 to AITC concentrations ≥ 1/50 vol/vol became paralyzed (highly intoxicated or dead) within 10 minutes
366 (Figure 1A, log-rank Mantel-Cox tests, $p<0.0001$). Thus, this rapid immobilization indicates that plant-
367 derived electrophilic compounds like AITC can have a strong negative effect on fly survival, consistent
368 with previous findings using volatile PITC (Lichtenstein et al. 1964).

369

370 **Volatile AITC is detected by Or42a in *D. melanogaster***

371 The high lethality caused by volatile AITC indicates that this volatile had the potential to be
372 detected by activating the fly's olfactory system, and that this could provide a fitness benefit if these
373 volatile toxins were then behaviorally avoided. To investigate this, we conducted exhaustive single
374 sensillum recordings (SSR) from the fly's olfactory organs, the antennae and maxillary palps, upon
375 stimulation with volatile AITC. Several OSNs showed excitatory responses to AITC, but OSNs in palp
376 basiconic (pb) sensilla (pb1a) were the most strongly activated (Figure 1 B-C, 113.8 ± 10.4 spikes/sec
377 from pb1a, n=8). Because previous studies reported that *D. melanogaster* pb1a OSNs express *Or42a*
378 (Couto et al. 2005), we investigated whether AITC responses in pb1a OSNs are indeed mediated by
379 Or42a. OSNs in pb1 sensilla from control flies showed strong responses to volatile AITC (Figure 1D,
380 Canton-S flies: 119.3 ± 10.8 spikes/sec, n=9; w^{1118} flies: 126.7 ± 9.8 spikes/sec, n=6). In contrast,
381 ONSs in pb1 sensilla from *Or42a* null mutant flies showed no response (-1.6 ±1.74 spikes/sec, n=6;
382 Kruskal-Wallis test with Dunn's multiple comparison, $p<0.05$ in both cases), suggesting that Or42a
383 detects volatile AITC in these sensilla. Furthermore, OSNs in pb1a of *TrpA1* null mutant flies still
384 responded to AITC, suggesting that the contact chemoreceptor TrpA1 is not necessary for maxillary
385 palp olfactory detection of this compound (Figure 1D, 152.7 ± 9.1 spikes/sec, n=6; $p>0.05$).

386

387 **Volatile AITC repels *D. melanogaster* via Or42a**

388 Next, we examined if activation of OSNs housing Or42a play a role at the behavioral level
389 (whole organism). Previous studies have shown that the presence of food-related odorants increase sugar
390 consumption in *D. melanogaster* (Reisenman and Scott, 2019). Based on this, we hypothesized that the

391 presence of aversive odorants such as AITC would decrease sugar consumption. To investigate this
392 hypothesis, we conducted consumption assays. In brief, groups of 10-15 food-deprived female flies were
393 offered 50 mM glucose water solution dyed blue in the presence or absence of volatile AITC (1:500
394 vol/vol loaded on filter paper), such as that flies could smell, but not contact, the AITC solution (Figure
395 supplement 1B). After 15 minutes flies were frozen and then the amount of blue dye in the abdomen of
396 each fly within a vial was quantified blind to treatment; these values were used to calculate a single
397 feeding score/vial (see materials and methods). We found that genetic background control flies and
398 wild-type Canton-S flies fed less when volatile AITC was present than in presence of the solvent control
399 (one-sample signed rank test on normalized data, $p<0.001$, $n=16$; Figure 1E). Although mutant flies still
400 fed less in presence than in absence of AITC volatiles ($p<0.05$, $n=14$), the reduction in consumption was
401 lower than that of the genetic control group (median normalized feeding scores: 0.35 and 0.83 in control
402 and mutant flies, respectively; $p<0.005$, Mann-Whitney U test). These results indicate that Or42a
403 mediates aversion to AITC in this behavioral context.

404 Additionally, we conducted a positional olfactory assay based on Ohashi and Sakai (2015), with
405 various modifications to prevent flies from physically contacting the odor source (Figure supplement
406 1C). Groups of 10-12 female flies were briefly ice-anesthetized and released at the juncture between the
407 two glass pipettes, allowing flies to choose between the pipette closest to the odor source (hereafter
408 referred to as "odorous side/tube", for simplicity) and the pipette closest to the solvent (control
409 side/odorless tube; Figure supplement 1C). The number of flies in each tube as well as in the middle
410 section where flies were released was counted every five minutes up to minute 35, and then again at 65
411 minutes in tests with AITC. We first confirmed that flies can show normal olfactory-guided behavior in
412 this behavioral set-up using apple cider vinegar, a well-established olfactory attractant (Semmelhack and
413 Wang 2009; Becher et al. 2010). Canton-S flies preferred the odorous tube from minute 20 onwards
414 (one-sample signed rank tests, $p<0.05$ in all cases, $p=0.09$ at minute 15, $n=21$). We then tested whether
415 and to what degree AITC causes olfactory repellence in this behavioral context. Genetic control flies and
416 wild-type Canton-S flies avoided the AITC tube at various time points (25, 30, 35 and 65 minutes in
417 genetic controls, one-sample signed rank tests, $p<0.005$ in all cases, $n=15$ Figure 1F; and from 25
418 minutes onwards in Canton-S, $p<0.05$ in all cases, $n=19$;), while *Or42a-/-* mutants only avoided the
419 AITC tube at the 65 minutes time point ($p<0.005$). These findings suggest that *Or42a* plays a crucial
420 role in mediating olfactory-driven behavioral aversion to AITC. Similar percentages of genetic control
421 and *Or42a-/-* mutants choose one or the other tube at all time points (the average of medians over all

422 time points were 79.7% and 82.5%, respectively; Mann-Whitney U tests, $p>0.05$ at all-time points;
423 Figure supplement 2C), suggesting that *Or42a-/-* mutants are as active as wild-type flies in presence of
424 AITC. We also confirmed that *Or42a-/-* mutants are capable of odor-mediated olfactory orientation. We
425 conducted dual-choice trap assays offering apple cider vinegar vs. water as described in Matsunaga et al.
426 (2019). About 50% (median) of flies released in each test (n=8, n=20 females/test) were trapped and of
427 these, 100% (median) were found in the odor-baited trap (Wilcoxon-matched pairs test, $p<0.005$, n=8).
428 This result confirms that the lack of behavioral aversion to AITC in *Or42a-/-* was not due to generalized
429 olfactory defect.

430 We also tested whether the *Or42a* olfactory circuit can *per se* mediate olfactory avoidance of
431 volatile AITC (Figure 1G). We conducted positional assays with *Orco* null mutant flies in which we
432 rescued the olfactory function specifically in the *Or42a* circuit. While the two parental control groups
433 (UAS-Orco, n=15, and Or42a-Gal4, n=16) distributed at random between the odorous and the control
434 tubes at all time points (one sample signed rank tests, $p>0.05$ in all cases), rescued flies (Or42a-Gal4>
435 UAS-Orco, n=13) significantly avoided the AITC tube from 15 minutes onwards ($p<0.05$ at 15, 20 and
436 25 minutes, $p<0.001$ at 30 and 35 minutes; tests stopped at 35 minutes). These results support the
437 hypothesis that Or42a OSNs in pb1a alone are sufficient to induce aversion to AITC.

438 It has been reported that Or42a mediates behavioral attraction towards fruit/fermentation
439 volatiles, including γ-hexalactone (Dweck et al. 2016). Thus, we used this odorant to test whether our
440 behavioral assays yielded results consistent with these previous findings. In consumption assays lasting
441 10 minutes, Canton-S flies increased their feeding in the presence of volatile γ-hexalactone 1:50 vol/vol
442 (normalized median=1.65, n=25, one-sample rank test, $p=0.001$), but this effect was lost in *Or42a-/-*
443 mutants (normalized median=0.89, n=24, $p=0.5$; Figure Supplement 2A). In the positional olfactory
444 assay, a larger proportion of genetic control flies than of *Or42a-/-* mutants choose either tube in
445 presence of 1:10 vol/vol γ-hexalactone (Figure Supplement 2D, range of medians for all time points:
446 91% and 50-89% in control and mutant flies, respectively; Mann-Whitney U tests, $p<0.05$ in all cases),
447 suggesting that the presence of the odor increases exploratory activity in control flies. Moreover, control
448 flies and wild-type Canton-S flies showed attraction to 1:10 vol/vol γ-hexalactone (at 20 and 30 minutes
449 in genetic control, n=19, and at 5, 10, and 15 minutes in Canton-S, n=12; one-sample signed rank tests,
450 $p<0.05$ in all cases), but this attraction was lost in *Or42a-/-* mutants (Figure supplement 1B). These
451 behavioral attraction phenotypes are consistent with the results reported by Dweck et al. (2017), and

452 with our findings showing that volatile γ-hexalactone did not negatively affect survival (Figure
453 supplement 1E).

454 Given that we found that Or42a participates in both mediating repellence to AITC and attraction
455 to γ-hexalactone, we next tested whether these two odorants activate additional OSNs. Through
456 exhaustive SSR from antennae and maxillary palps upon stimulation with γ-hexalactone, we found that
457 pb1a OSNs was the only olfactory sensillum activated by γ-hexalactone (Figure supplement 2F), while
458 AITC activated several additional OSN types (e.g. ab4a; Figure 1C). In sum, our data suggested that
459 activation of *Or42a*-positive-OSNs, along with other Or-expressing OSNs likely mediates behavioral
460 aversion, whereas the simultaneous activation of *Or42a*-positive-OSNs and other yet uncharacterized
461 olfactory circuits involving e.g. Ionotropic receptors (Benton et al. 2009) would mediate behavioral
462 attraction.

463

464 **Pb1a-like OSNs in Brassicales-specialists evolved broadened sensitivity to isothiocyanates (ITCs)**

465 We next investigated how the evolutionary transitions from microbe-feeding to herbivory have
466 affected OSNs, using the reference species *D. melanogaster* as well as species within *Scaptomyza*: the
467 microbivorous *S. hsui* and *S. pallida,* and the herbivorous Brassicales specialists *S. flava* and *S. montana*
468 (Kim et al. 2021; Peláez et al. 2023). We investigated whether *Scaptomyza* species have pb1-like
469 sensilla homologous to *D. melanogaster* pb1 and if so, the extent to which they respond to a broader
470 range of ITC compounds, since Brassicales plants release ITCs upon wounding (MacLeod et al. 1989;
471 Cuellar-Nuñez et al. 2022).

472 We first validated our methods for functional characterization of sensilla in *D. melanogaster*. We
473 used compounds that serve as diagnostic for the three sensilla types found in the maxillary palps of *D.*
474 *melanogaster* (see methods for details). In addition, we used as stimuli *trans*-2-hexenal, 2-hexanol,
475 methyl salicylate, 2-heptanone and phenethyl alcohol, and Brassicales-derived isothiocyanates (ITCs)
476 including allyl ITC (AITC), isobutyl ITC (IBITC), butyl ITC (BITC), sec-butyl ITC (SBITC), and
477 phenethyl ITC (PITC). Using the diagnostic odorants, we confirmed the presence of three different types
478 of palp sensilla (pb1, pb2 and pb3) in *D. melanogaster*. We also found that *Dmel* pb1a OSNs were
479 activated by AITC (128.3 ± 10.8 spikes/sec, n=9), but not by the other ITCs tested (<10 spikes/sec,
480 Figure 2).

481 We next characterized OSNs in pb sensilla in four *Scaptomyza* species and used the spike rate to
482 determine if data clustered by sensilla type (Figure 2, Figure supplement 3A). In all species, the sensilla
483 fell into three functional classes similar to *Dmel* pb1, pb2 and pb3, which we termed pb1-like, pb2-like,
484 and pb3-like. The response profiles of *Scaptomyza* pb3-like OSNs were different from those of *Dmel*
485 pb3, likely because the homologs of *Or59c* and *Or85d*, which are respectively expressed in *Dmel* pb3a
486 and p3b, are unidentified in the genomes of *Scaptomyza* (Goldman-Huertas et al. 2015). We found two
487 types of pb1-like sensilla in the four *Scaptomyza* species, each of which exhibited an odorant tuning
488 pattern similar to that of *Dmel* pb1a. However, only one subset of *Scaptomyza* pb1b-like sensilla
489 exhibited an odorant tuning pattern similar to that of *Dmel* pb1b, while the other subset showed
490 subthreshold activity and thus was excluded from analysis. As in *Dmel*, AITC activated pb1a-like
491 sensilla in all four *Scaptomyza* species (Figure 2). Notably, several other ITCs, including IBITC, BITC,
492 and SBITC, additionally activated *S. flava* (*Sfla*) and *S. montana* (*Smon*) pb1a-like OSNs (the average #
493 of spikes/second ranged from 30.3 to 107.3 across ITCs in *Sfla* pb1a-like, and 48.3 to 110.3 in *Smon*
494 pb1a-like, n=6/ITC and species; Figure 2). Methyl salicylate activated all *Scaptomyza* pb2b-like sensilla
495 but not *Dmel* pb2b (the average spike rates across *Scaptomyza* pb1a-like ranged from 70 to 110.7
496 spikes/second, n=6-7, compared to 11.6 ± 4.4 spikes/second for *Dmel* pb2b, n=9; Figure 2) and
497 interestingly, this compound is a known *S. flava* volatile attractant in natural settings (Orre et al. 2010).
498 Furthermore, the odorant response profiles of OSNs in pb3-like sensilla were more similar between the
499 more distantly related species *S. hsui* and *S. pallida,* than between the more closely related species *S.*
500 *pallida* and *S. flava,* or *S. pallida* and *S. montana.* For example, *trans*-2-hexenal activated *Shsu* and *Spal*
501 OSNs in pb3a-like sensilla but not OSNs of *Sfla* or *Smon* in pb3a-like sensilla, while phenethyl acetate
502 activated *Sfla* and *Smon* OSNs in pb3a-like but not those of *Shsu* or *Spal* pb3a-like sensilla (Figure
503 supplement 3B-C). Thus, niche differences rather than phylogenetic distance may explain the functional
504 divergence between OSNs in maxillary palp sensilla in these *Scaptomyza* species.

505

506 **Brassicales specialists have a higher number of pb1-like sensilla.**

507 We next generated anatomical maps of sensilla on the anterior part of the maxillary palps of the
508 species of *Scaptomyza* and of *D. melanogaster* for comparison, using diagnostic chemicals (Figures 3A,
509 Figure supplement 4, Supplementary file 10; see methods for more detail). Interestingly, while *D.*
510 *melanogaster* had a relatively randomized distribution of sensilla on the palps, consistent with previous

511 reports (de Bruyne et al. 1999), all four *Scaptomyza* species exhibited a more organized sensilla pattern,
512 with pb1-like, pb2-like, and pb3-like respectively located medially, distally, and proximally as was
513 indicated in *D. mojavensis* (Crowley-Gall et al. 2016).

514 The proportions of each type of palp sensilla varied within and between species (Figure 3A and
515 Figure supplement 4). *S. flava* had a larger number of pb1-like sensilla (22.3 ± 1.5, average ± SEM) than
516 of pb2-like (3.7 ± 0.3) or pb3-like sensilla (12.3 ± 1.2; ANOVA with Holm-Šídák's multiple
517 comparisons test, $p<0.0001$ and $p<0.001$). *S. montana* also had a higher number of pb1-like sensilla (17
518 ± 2.3 pb1-like, 6.3 ± 1.2 pb2-like and 5.6 ± 0.7 pb3-like sensilla; $p<0.01$ in both cases). In contrast, *D.*
519 *melanogaster* and the other two *Scaptomyza* species had similar numbers of each sensilla type (range:
520 5.6-7.3 pb sensilla in *D. melanogaster*, 4.3-6.6 in *S. hsui*, and 7.3-10.7 in *S. pallida;* $p>0.05$ for the three
521 species). These findings suggest an expansion of pb1-like sensilla in Brassicales specialists over the
522 course of evolution. Moreover, *S. flava* and *S. montana* had an overall larger number of olfactory
523 sensilla on the palps (38.3 ± 0.3 and 29 ± 2.1 pb sensilla, respectively) compared to *D. melanogaster* (20
524 ± 1.2)*, S. hsui* (15.3 ± 0.9), and *S. pallida* (26.3 ± 3.0) (Figure 3A). The largest number of palp sensilla
525 in *S. flava* correlated with the larger size of their palps within *Scaptomyza*: the surface area of one palp
526 of *S. flava* was 3.57 ± 0.32 mm^2, while that of *S. hsui* and *S. pallida* were respectively 2.37 ± 0.23 mm^2
527 and 2.00 ± 0.18 mm^2; the surface area of the maxillary palp of *D. melanogaster* was 2.99 ± 0.41 mm^2
528 (Figure supplement 5). Taken together, these results show that Brassicales plant specialists have a higher
529 proportion of pb1-like sensilla compared to microbe-feeding *Drosophila* and *Scaptomyza*, suggesting
530 that Brassicales plant specialist *Scaptomyza* species may have enhanced capacity to detect volatile ITCs.

531

532 ***Sfla Or42a* is triplicated in the genome of *S. flava* and is highly expressed in the maxillary palps.**

533 We next investigated the expression of *Or* genes in the OSNs of sensilla in the maxillary palps
534 across some of the species of interest. Initially, we scanned the known genome sequences of species in
535 the genus *Scaptomyza* and found a duplication of *Or42a* in the lineage leading to all known *Scaptomyza*,
536 while the *D. melanogaster* outgroup had a single *Or42a* homolog (Figure supplement 6). Interestingly,
537 within *Scaptomyza*, *S. flava* exhibited serial triplicates in one of the *Or42a* duplicates, which we named
538 *Or42a2*, *Or42a3*, and *Or42a4* (Figure 3B and Figure supplement 6), whereas *S. montana* retained only
539 two paralogs, like *S. hsui* and *S. pallida*.

540 To determine the extent of *Or* gene expression, including that of the paralogs of *Or42a*s in the
541 *Scaptomyza* maxillary palps, we conducted species- and sex-specific RNA transcriptome analyses of *S.*
542 *pallida* and *S. flava* (Figure 3C; Figure supplement 7). We confirmed the expression of *Spal Or42a* and
543 *Sfla Or42a2-4* in the palps. Interestingly, the *Sfla Or42a* paralogs were each expressed at levels
544 comparable to those of other *Or* genes, such as *Or33c*, the homolog of which in *D. melanogaster* is
545 expressed in OSNs of pb2a sensilla (see below). Furthermore, we confirmed the expression of homologs
546 *Or71a* (expressed in OSNs of *Dmel* pb1b), and of *Or33c/Or85e* and *Or46a* (expressed in OSNs of *Dmel*
547 pb2a and pb2b) in both *Spal* and *Sfla* palps. Only *Spal Or42a2* and *Sfla Or42a2-4* were expressed in the
548 OSNs of their respective palp sensilla (pb1-like), whereas *Spal Or42a1* and *Sfla Or42a1* were not.
549 *Or85d* and *Or59c* were respectively expressed in OSNs of *Dmel* pb3a and pb3b but the homologs were
550 unidentified in the genomes of *Scaptomyza* (Goldman-Huertas et al., 2015). Instead, *Or59a1, Or67a1,*
551 *Or67a2,* and *OrN2a* were strongly expressed in OSNs of both *Spal* and *Sfla,* suggesting that these
552 homologs may be expressed in pb3a or pb3b (Figure 3C). In summary, potential conservation of *Or*
553 expression in pb1 and in pb2 sensilla, and the difference in *Or* expression in OSNs of pb3 between
554 *Drosophila* and *Scaptomyza,* may reflect the similarities and differences in their odorant response
555 profiles (See Figure 2).
556

557 **Brassicales specialists have more abundant *Or42a*-positive-OSNs OSNs.**

558 Our transcriptome analysis revealed high expression of *Or42a* triplicates in *Sfla* maxillary palps
559 (Figure 3C), which could be due to high expression of *Or42a* in individual cells and/or a higher number
560 of *Or42a*-positive-OSNs. To distinguish between these possibilities, we quantified the number of
561 *Or42a*-positive-OSNs in the maxillary palps of *Sfla* and *Spal* using hybridization chain reaction RNA
562 fluorescent in situ hybridization (HCR RNA FISH). Due to the high sequence similarity between the
563 paralogs, we designed an RNA probe based on the conserved sequence region of *Sfla Or42a2-4* to
564 visualize all *Or42a2-4* paralog^{+} cells in *S. flava.* Similarly, we designed the *Spal Or42a2* probe to
565 compare the expression of homologs in the maxillary palps of *Sfla* and *Spal* (Figure 3B).

566 HCR RNA FISH analysis revealed that the maxillary palps of *S. flava* contained more *Or42a*-
567 positive-OSNs than those of *S. pallida,* as well as more *Orco*-positive-OSNs (*Or42a*-positive-OSNs:
568 34.2 ± 1.53 in *S. flava* vs 13.8 ± 0.74 in *S. pallida*, average ± SEM; *Orco*-positive-OSNs: 96.4 ±
569 1.91 in *S. flava* vs 53.2 ± 3.00 in *S. pallida*, Mann Whitney U-tests, $p<0.01$ in both cases, n=5/species,

570 Figure 3D-E). Additionally, the ratio of the total number of *Or42a*-positive-OSNs to the total number of
571 *Orco*-positive-OSNs was higher in *S. flava* (35.6 ± 1.83 % in *S. flava* vs 26.2 ± 1.86 % in *S. pallida*,
572 $p<0.01$, Figure 3F). This indicates that *S. flava* not only has more *Or42a*-positive-OSNs and *Orco*-
573 positive-OSNs, but also a greater proportion of *Or42a*-positive-OSNs relative to the overall number of
574 OSNs in the maxillary palps.

575

576 **Paralog-specific functional evolution of Or42a.**

577 We next investigated the functional evolution of *Or42a* triplicates in *S. flava*. To do this, we
578 expressed *Dmel Or42a, Spal Or42a2,* and *Sfla Or42a2-4* in *Dmel* antennal trichoid 1 (at1) OSNs in the
579 background of a null mutation for *Or67d*, the at1 cognate receptor (Kurtovic et al. 2007). We then
580 conducted SSR from at1 using six different odorant stimuli at 1/100 vol/vol: *trans*-2-hexenal, AITC,
581 IBITC, BITC, SBITC, and γ-hexalactone. We found that γ-hexalactone, *trans*-2-hexenal, and AITC
582 strongly activated OSNs expressing *Dmel* Or42a (range: 79-110 spikes/second) or *Spal* Or42a2 (range:
583 96-205 spikes/sec; Figure 4A-B), while IBITC, BITC and SBITC evoked much weaker responses from
584 these two paralogs (respectively 4.3-11 spikes/sec and 18.3-42.3 spikes/sec). In contrast, OSNs
585 expressing *Sfla* Or42a3 or *Sfla* Or42a4 were very sensitive to IBITC and BITC (range: 87-96.7
586 spikes/sec in *Sfla* Or42a3; 46-77.7 spikes/sec in *Sfla* Or42a4), which is consistent with the response
587 profiles of OSNs from wild-type *Sfla* pb1a (Figure 2). Notably, OSNs expressing *Sfla* Or42a4 showed
588 only small responses to γ-hexalactone. *Sfla* Or42a2 was only activated by AITC. These results align
589 with the niche difference between microbe-feeding flies and Brassicales specialists. Moreover, our
590 findings reveal the paralog-specific functional evolution of Or42a triplicates in *S. flava*, as different
591 paralogs have evolved distinct sensitivities to various ITC chemicals and fruit odors.

592 We also stimulated OSNs in pb1a (or pb1a-like) sensilla from the microbe-feeding species (*D.*
593 *melanogaster, S. hsui* and *S. pallida*) and the Brassicales specialists (*S. flava* and *S. montana*) with
594 various concentrations of odorants from 10^{-5} to 10^{-2} vol/vol. We calculated the odorant concentration
595 required to elicit a biological response halfway between the baseline and the maximum (50% effective
596 concentration values, EC_{50}) (Figure supplement 8). The EC_{50} values for γ-hexalactone were consistently
597 lower in the microbe-feeding species in comparison with the Brassicales specialists, indicating a lower
598 sensitivity to γ-hexalactone in the latter. All species had similar EC_{50} values for AITC. OSNs expressing
599 *Sfla* pb1a exhibited a lower EC_{50} value for *trans*-2-hexenal compared to those expressing *Smon* pb1a

600 and the other microbe-feeding species. This heightened sensitivity to this general leaf odor in OSNs of
601 *Sfla* pb1a aligns with its potentially broader host range, as *S. flava* can be reared on plants from other
602 lineages in addition to Brassicales, such as Fabaceae or even Caryophyllaceae in New Zealand (Martin
603 2004)Maca 1972), whereas *S. montana* appears to be more restricted to Brassicaceae within the
604 Brassicales.

605

606 **AlphaFold2-led screening with ectopic expression of *Sfla* Or42a reveals the molecular changes**
607 **underlying changes in odor sensitivity**

608 We investigated which amino acid substitutions in *Sfla* O42a3 lead to the respective gain and
609 loss of sensitivity to BITC and γ-hexalactone in *Sfla* Or42a4 (there are total of 32 amino acid differences
610 between *Sfla* Or42a3 and *Sfla* Or42a4, Figure supplement 9A). For this, we predicted the 3D structures
611 of *Sfla* Or42a3 and *Sfla* Or42a4 in the cell membrane and aligned them in 3D space using PyMol, and
612 checked the overlap between Ors (Jumper et al. 2021; Mirdita et al. 2022; Benton and Himmel 2023;
613 Himmel et al. 2023).

614 One of the most striking differences in 3D structures between *Sfla* Or42a3 and *Sfla* Or42a4 was
615 observed in the S5 and S6 helices in the transmembrane region, which are reported to contain the ligand
616 binding pockets (Figure 4C and Figure supplement 9B; (Del Mármol et al. 2021; Zhao et al. 2024). We
617 therefore substituted each of the 32 amino acids in *Sfla Or42a4* individually with the corresponding
618 residues from *Sfla* Or42a3 *in silico,* predicted the 3D structures of the chimeras, and aligned them with
619 *Sfla* Or42a4 in 3D space until the local structural differences were resolved. The substitutions of A181D
620 and S307P in *Sfla* Or42a3 (hereafter referred to as A181D S307P) resolved the structural differences and
621 overlapped with *Sfla* Or42a4 in 3D space (Figure 4C and Figure Supplement 9B).

622 We then investigated whether these two amino acid substitutions could account for the *Sfla*
623 Or42a4 enhanced sensitivity to BITC and reduced sensitivity to γ-hexalactone, in comparison with *Sfla*
624 Or42a3. Using the *D. melanogaster* at1 empty neuron system, we functionally characterized the A181D
625 S307P variant, and found that the BITC to γ-hexalactone response ratio (net number of spikes evoked by
626 BITC divided by the sum of the net number of spikes evoked by BITC and γ-hexalactone) was greater
627 than *Sfla* Or42a3 and A181D S307P (Figure 4E-F; Mann-Whitney U test, $p<0.001$), but not between
628 *Sfla* Or42a4 and A181D S307P ($p>0.05$). This suggests that the two amino acid substitutions are

629 sufficient to increase the BITC to γ-hexalactone response ratio, by respectively increasing and reducing
630 the sensitivity to BITC and γ-hexalactone in *Sfla* Or42a4. This effect was observed in flies carrying the
631 heterozygous genotype A181D S307P/+ but not in flies with the homozygous A181D S307P genotype
632 (Compare Figure 4E-F with Figure supplement 10). Given that the focal gene is more highly expressed
633 in homozygous flies than in heterologous flies, it is possible that the OSNs' response to both BITC and
634 γ-hexalactone reached saturation in homozygous flies, obscuring further differences in spike ratios. In
635 summary, our findings demonstrate that A181D and S307P substitutions are critical for shifting the
636 receptor's sensitivity from fruit odorants to ITCs.

637

638

639 **DISCUSSION:**

640 In this study, we discovered that plant-derived ITCs have a detrimental effect on survival of *D.*
641 *melanogaster* through volatile exposure. We then found that volatile ITCs are detected by Or42a, which
642 is expressed in the maxillary palps, and that this Or is necessary for the behavioral aversion behavior to
643 volatile ITCs. To our knowledge, Or42a is the first known ITC olfactory detector in *D. melanogaster*.
644 Thus, these results suggest that Or42a works in combination with the "wasabi" taste receptor" TrpA1
645 and Painless to facilitate adaptive behavioral avoidance of these chemicals in *D. melanogaster* (Al-Anzi
646 et al. 2006; Kang et al. 2010; Mandel et al. 2018). We also conducted molecular evolutionary analyses,
647 site-directed mutagenesis, and functional assays to uncover the molecular mechanisms by which the
648 Brassicales specialist *S. flava* evolved paralogous copies of the homologous *Or42a* genes that we found
649 respond to a broad range of electrophilic compounds emitted by their host plants. Overall, our findings
650 provide new insight into the olfactory mechanisms that allow generalist insects to avoid lethal volatile
651 toxins and into the rapid evolution of an expanded set of more finely tuned *Or*s in specialist insects that
652 detect these volatile host-plant signals.

653 **Plant-derived volatile AITC is toxic to *D. melanogaster* and its detection and avoidance is**
654 **mediated by *Or42a*-positive-OSNs**

655 Plants have evolved a diverse array of specialized metabolites that repel or intoxicate insects
656 (Ibanez et al. 2012). Among these, plant-derived electrophilic compounds, including *trans*-2-hexenal
657 and ITCs, are highly reactive (Noge and Becerra 2015; Tocmo et al. 2021). For example, AITC derived

658 from wasabi and other mustard and Brassicales plants causes a highly pungent sensation in humans (Bell
659 et al. 2018). Additionally, ITCs exert toxic effects acutely on insects when volatilized as well
660 (Lichtenstein et al. 1964). Here, we found that volatile AITC also exerts a dose-dependent detrimental
661 effect on *D. melanogaster* adults (Figure 1A). As little as 10 minutes of exposure of low to moderate
662 concentrations of volatile AITC is sufficient to immobilize flies, underscoring the high toxicity of this
663 compound. These findings are consistent with previous findings showing that ingestion of AITC
664 decreases fly survival (Zimmermann et al. 2024) and with earlier studies on the toxic effect of volatile
665 PITC (Lichtenstein et al. 1964).

666 While TrpA1 pain receptors in *D. melanogaster* mediate the detection of ITCs and other reactive
667 compounds by taste as they do in humans (i.e, by contact, (Kim et al. 2010)), it was unclear whether and
668 to what degree insects have evolved strategies to avoid these compounds via olfaction. Our findings
669 demonstrate that Or42a and its associated OSNs are key components in detecting and inducing olfactory
670 aversion to AITC in *D. melanogaster*, as revealed through exhaustive SSR and olfactory behavioral
671 assays (Figure 1). We found that maxillary palp pb1a OSNs, which express Or42a, respond strongly to
672 olfactory stimulation with AITC in wild-type *D. melanogaster* and TrpA1^{-} loss of function mutants.
673 However, this response was absent in *Or42a-/-* mutants, demonstrating that Or42a is necessary for
674 detecting volatile AITC in pb1a OSNs (Figure 1C-D). Using two different behavioral assays, we found
675 that volatile AITC induces strong behavioral aversion in wild-type and genetic control *D. melanogaster*
676 lines. These flies consumed less sugar solution than *Or42a-/-* mutant flies in presence of volatile AITC,
677 indicating that this compound causes olfactory aversion in a feeding context (Figure 1E). Furthermore,
678 control flies avoided volatile AITC in the positional behavioral assay, while *Or42a-/-* mutants only
679 showed aversion after a long-time exposure (65 minutes) (Figure 1F). The delayed avoidance in *Or42a-*
680 */-* mutants could be due to the involvement of additional circuits mediating the aversion to volatile
681 AITC, such as Or7a, which is expressed in ab4a OSNs and was also activated by volatile AITC (Figure
682 1C), and/or to undescribed olfactory ionotropic receptors that may also respond to AITC. Alternatively,
683 AITC might have adhered to the internal surface of the glass tube during the course of the experiment,
684 leading to taste-mediated aversion via TrpA1.

685 Dweck et al., (2015) reported that *Dmel* Or42a detects fruit odors and mediates behavioral
686 attraction to these odors. We confirmed this result in our hands by showing that the fruit odor γ-
687 hexalactone strongly activates *Or42a*-positive-OSNs (Figure 4A-B, Figure supplement 2). Moreover,

688 the presence of this odor increased consumption of sugar and induced positional behavioral attraction in
689 control flies, but not in *Or42a-/-* mutants (Figure Supplement 2A-B). These findings may appear
690 contradictory: a single OSN type (*Or42a*-positive-OSNs) mediates aversion to AITC while also driving
691 attraction to γ-hexalactone. This paradox could be resolved considering different levels of OSNs
692 activation, which may result in the recruitment of alternative combinations of glomeruli that are
693 activated by interglomerular local neurons (Kreher et al. 2008; Semmelhack and Wang 2009; Mohamed
694 et al. 2019). Alternatively, distinct subsets of OSNs may be activated by different odorants, leading to
695 behavioral responses of opposite valence (Haverkamp et al. 2018), or a combination of both mechanisms
696 may be involved. Indeed, we found that rescue of Orco-mediated olfactory function specifically in
697 *Or42a*-positive-OSNs was sufficient to induce repellence to AITC (Figure 1G). Additionally, we found
698 that AITC induced the strongest responses in pb1a OSNs but also elicited spiking activity in other OSNs
699 such as ab4a and ab8b, albeit to a lesser degree (Figure 1C). In contrast, γ-hexalactone activated only
700 pb1a OSNs (Figure Supplement 2F). Thus, it's possible that the combined activation of pb1a OSNs
701 along with ab4a and/or ab8a OSNs leads to repellence, while activation of pb1a OSNs, possibly
702 alongside other uncharacterized OSNs, results in behavioral attraction. Further research is needed to
703 fully elucidate the mechanisms by which a single OSN type may mediate behavioral aversion to one
704 ligand while driving attraction to another.

705

706 **Functional evolution of *Or42a* and *Or67b* in *Scaptomyza* mustard plant specialists**

707 Phylogenetic evidence and ancestral state reconstruction indicate that the ancestor of all
708 herbivorous *Scaptomyza* (subgenus *Scaptomyza*) diverged from a microbe-feeding common ancestor and
709 evolved the herbivory habit ca. 10-15 million years ago, giving rise to a monophyletic Brassicales-
710 specialized lineage that includes *S. flava* and *S. montana,* and a Carophyllales-feeding lineage that
711 includes *S. graminum* (Goldman-Huertas et al. 2015; Kim et al. 2021; Peláez et al. 2023). This pattern of
712 specialization on plants that release specialized metabolites that are toxic to many other insects provides
713 a novel niche for host use (Ali and Agrawal 2012), given that specialists also evolved mechanisms to
714 detoxify plant toxins (Gloss et al. 2014; Karageorgi et al. 2019), and may help insects escape pressure
715 from natural enemies like parasitoids (Bernays and Graham 1988). Indeed, drosophilids, including *D.*
716 *melanogaster*, and *S. flava* use the mercapturic acid pathway to detoxify ITCs (Gloss et al. 2014).
717 Notably, the detoxification enzymes that catalyze this pathway in *S. flava* exhibit a 10-fold higher

718 catalytic efficiency *in vitro* for ITCs compared to other flies, likely allowing them to thrive on
719 Brassicales plants (Gloss et al. 2019).

720 Specialized insects also often use these toxic compounds as olfactory "tokens" to find their
721 hostplants. Many Brassicales plants release species-specific volatile ITCs (Wu et al. 2021) at particular
722 ratios and concentrations that attract a guild of specialized herbivores through olfaction. For instance,
723 the mustard specialist diamondback moth *Plutella xylostella* uses volatile ITCs to find suitable
724 oviposition sites (Liu et al. 2020). Volatile ITCs are also known to attract *S. flava* females at least in
725 laboratory tests (Matsunaga et al., 2021), and the herbivorous *Scaptomyza* have lost four *Or* that are
726 involved in attraction to yeast-associated volatiles in *D. melanogaster* (Goldman-Huertas et al. 2015;
727 Matsunaga et al. 2021). Given the need for finer olfactory resolution in mustard plant specialist like *S.*
728 *flava*, we investigated whether the *Or42a* homologs and the Ors they encode in this lineage have
729 undergone differentiation and specialization compared to those of more generalist microbe-feeding
730 species like *D. melanogaster* as well as closer relatives of the herbivorous *Scaptomyza*, which include
731 the microbivores *S. hsui* and *S. pallida*.

732 To address this question, we started by constructing functional maps of the palp olfactory
733 sensilla across five species that spanned both Brassicales-feeding and microbe-feeding *Scaptomyza*
734 (Figure 2 and 3A, Figure Supplement 3). Our analysis confirmed that *Scaptomyza* species possess three
735 distinct types of sensilla, similar to those found in *D. melanogaster* (Ray et al. 2008; Dweck et al. 2016).
736 We found that the overall tuning patterns were largely conserved between *Scaptomyza* and *Drosophila*,
737 with the exception of OSN responses in pb3a- and pb3b-like sensilla (Figure 2). While OSNs housed in
738 pb1a sensilla from all microbivore and herbivorous species responded to volatile AITC, only OSNs
739 housed in *Sfla* pb1a-like and *Smon* pb1a-like sensilla additionally responded to other volatile ITCs
740 (Figure 2).

741 Next, we investigated the odor-response profiles of the Or42a paralogous genes. We previously
742 found that triplicated and positively selected *Sfla* Or67b is expressed in antennal OSNs and responds to
743 aromatic and some aliphatic ITCs in a paralog-specific manner. However, all three Or67b paralogs
744 showed a poor response to organosulfur ITCs, including AITC. The *D. melanogaster* and *S. pallida*
745 Or67b copies did not respond to any volatile ITCs (Matsunaga et al. 2021). In this study, on the other
746 hand, we found that all three Or42a paralogs in the Brassicales-feeding species of *Scaptomyza*
747 responded to organosulfur ITCs such as AITC (Figure 4B). Thus, the gene duplications and amino acid

748 substitutions of *Or42a*, along with those of *Or67b*, likely play a crucial role in enabling Brassicales-
749 plant specialist *Scaptomyza* species to detect a wide range of ITCs, including specific blend ratios and
750 concentrations, facilitating effective host plant location. Further refinement could be achieved by
751 changes in processing in downstream olfactory centers, such as those recently reported in the noni
752 specialist *D. sechellia* (Auer et al. 2020).

753 *Or67b* in *S. flava* is primarily expressed in the antennae (Matsunaga et al. 2021), whereas *Or42a*
754 is expressed in the maxillary palps (Figure 3C). In *D. melanogaster*, OSNs from the maxillary palps
755 have lower sensitivity thresholds to certain host-related compounds compared to antennal OSNs (Dweck
756 et al. 2016). Indeed, we found that the *Sfla* Or42a paralogs are much more sensitive to AITC than its
757 Or67b paralogs [Figure 4, (Matsunaga et al. 2021)]. Odor response redundancy between antennal and
758 maxillary palp Ors could have evolved to further underpin olfactory orientation over both long and short
759 distances in drosophilids (Dweck et al. 2016). Given the proximity of Or42a OSNs to the mouthparts,
760 their activation could potentially modulate feeding behaviors, as suggested in *D. melanogaster* (Shiraiwa
761 2008). *S. flava* and *S. montana* adult females feed on the juice that seeps into the leaf wounds they create
762 in Brassicales plants before oviposition (Peláez et al. 2022). Given this stereotyped feeding behavior of
763 adult females, while the activation of contact chemoreceptors by ITCs could help females assess the
764 suitability of an oviposition site through taste, flies may also be aided by olfactory activation via the
765 maxillary palps perhaps even before tasting the plants.

766 **Differential expression of *Or*s in *Scaptomyza***

767 Our maxillary palp RNA-seq expression data (Figure 3C), combined with electrophysiological
768 results showing similar patterns of odor responses in pb1-like and pb2-like sensilla OSNs (Figure 2),
769 suggest that all *Scaptomyza* species express the following *Or*s in the OSNs of pb sensilla: *Or42a* in
770 pb1a-like, *Or71a* in pb1b-like, *Or33c* and *Or85e* in pb2a-like, and *Or46a* in pb2b-like. This raises the
771 question of which *Or*s are expressed in OSNs of pb3a- and pb3b-like sensilla in *Scaptomyza*. Based on
772 our RNA-seq data, candidates included *Or67a, Or98b, Or59a,* and *OrN2a*, as they were robustly
773 expressed in the maxillary palps (Figure 3C). Among these, only Or67a has been functionally
774 characterized in *D. melanogaster*, and responds to 2-heptanone (Auer et al. 2020). Our SSR experiments
775 showed that 2-heptanone also activated OSNs in pb3a-like (Figure 2), raising the possibility that
776 *Scaptomyza* pb3a-like OSNs express Or67a. Alternatively, other yet uncharacterized Ors responsive to
777 2-heptanone might be expressed in these OSNs.

778 Using HCR RNA FISH, we discovered an increase in the number of *Or42a*-positive-OSNs in *S.*
779 *flava* compared to *S. pallida* (Figure 3C). Similar increases in OSNs which detect odors that bear
780 biological significance for insects have been reported in several *Drosophila* species. For instance, the
781 noni fruit specialist *D. sechellia* and the seasonal specialist of *Pandanus* spp. screw pine fruits *D. erecta*
782 both show an increase in the number of *Or22a*$^{+}$ OSNs (Dekker et al. 2006; Linz et al. 2013; Auer et al.
783 2020). These increases in OSNs have been shown to enhance odor tracking by reducing adaptation in
784 projection neurons in *D. sechellia* (Takagi et al. 2024). We hypothesize that the increase in the number
785 of *Or42a*-positive-OSNs in *S. flava* may similarly contribute to enhance odor sensitivity and tracking
786 during host plant finding, which will require further investigation to address.

787 **Insight into the binding pocket of Or42a paralogs**

788 Our results demonstrated that the Or42a paralogs from microbe-feeding species show strong
789 responses to both AITC and γ-hexalactone (Figure 4), while the paralogs from the herbivorous *S. flava*
790 show a notable shift in olfactory sensitivity. For example, *Sfla* Or42a3 showed moderate responses to γ-
791 hexalactone (about an order of magnitude lower than those of the Or42a from the microbe-feeding *S.*
792 *pallida*), and *Sfla Or42a4* showed even less spiking activity (Figure 4D-E). Intriguingly, *Sfla* Or42a4
793 has a relatively higher sensitivity to BITC compared to Or42a3 (Figure 4B, D and E). These findings
794 align with the fact that *S. flava* has undergone a full transition to the herbivory habit. To explore the
795 mechanisms underlying this shift from fruit-detector to ITC-detector, we employed computational and
796 functional approaches to identify the amino acid substitutions responsible for the differences in odor
797 sensitivities between *Sfla* Or42a3 and Or42a4.

798 The binding pocket of Ors is located within the transmembrane region, and amino acid
799 substitutions in these regions can alter the ligand's binding affinity [(Del Mármol et al. 2021; Zhao et al.
800 2024), although extracellular loops are also suggested to play an important role (Carraher et al. 2015)].
801 Our AlphaFold2-led screening for amino acid substitutions identified two key substitutions in the
802 transmembrane portion: A181D and S307P (Figure 4C). We substituted these two amino acids and
803 found that OSNs expressing this chimeric Or increased the BITC to γ-hexalactone response ratio, by
804 respectively increasing and reducing the sensitivity to BITC and γ-hexalactone (Figure 4E-F). The
805 substitution of serine to proline (S307P) alters both the charge and the protein structure, which likely
806 accounts for the impact in the notable change in ligand sensitivity. However, the increased BITC to γ-
807 hexalactone spike ratio for was observed only in flies heterozygous for A181D and S307P (Or67d^{Gal4};

808 UAS-A181D S307P/+) and not in the flies homozygous for A181D and S307P (Figure Supplement 10).
809 Given that homozygous flies express A181D and S307P more strongly than the heterozygous flies, it is
810 possible that the OSNs response to both BITC and γ-hexalactone reached saturation in homozygous
811 flies, obscuring further differences in spike ratios. Alternatively, excessive expression of A181D and
812 S307P in cells may have altered the 3D structure of the protein, reverting it closer to the original *Sfla*
813 Or42a3 conformation and restoring the original binding pocket. Nonetheless, the partial rescue we
814 observed in heterologous flies indicates that A181D and S307P are critical for altering the binding
815 pocket structure, enabling the binding pocket of Ors to better accommodate BITC instead of γ-
816 hexalactone.

817

818 **CONCLUSIONS:**

819 Taken together, our study reveals that generalist insects have evolved olfactory sensory
820 mechanisms that allow them to detect and avoid plant-derived volatile electrophilic toxins, such as ITCs.
821 In contrast, Brassicales plant specialists have undergone significant evolutionary sensory adaptations for
822 host recognition, including specialized ITC olfactory receptors to aid host plant location. These
823 adaptations involve the triplication of homologous Ors in the antennae (Matsunaga et al. 2021), as well
824 as in the maxillary palps (this study), which collectively expanded the sensitivity and detection range for
825 these and other signature hostplant odorants. Furthermore, our use of AlphaFold2, followed by site-
826 directed mutagenesis and electrophysiology, identified critical amino acid changes for the evolution of
827 specialized odorant receptors. This also demonstrates the utility of machine learning algorithms in
828 evolutionary biology research, particularly in screening and identifying functionally relevant genetic
829 changes for follow-up functional studies.

830

831 **ACKNOWLEDGEMENTS:**

832 We are grateful to Bloomington Drosophila Stock Center, and Drosophila Genomics Resource Center
833 (NIH Grant 2P40OD010949). T.M. thanks Dr. Akinao Nose and Dr. Hiroshi Kohsaka for advice and
834 encouragement, and the members of Nose' laboratory for discussions. We thank members of the
835 Whiteman and Scott Laboratories for discussions and comments on the manuscript. This work was
836 supported by the Grant-in-Aid for Scientific Research Activity Start-up (T.M.), the Uehara Memorial

Foundation (award number 201931028 to T.M.), the National Institutes of Health (NIH) Grant (award number R35GM139653 to Gary Karpen), and the National Institute of General Medical Sciences of the NIH (award number R35GM119816 to N.K.W.).

FIGURE CAPTIONS:

Figure 1: *Drosophila melanogaster* Or42a mediates volatile toxicity of allyl isothiocyanate (AITC) and behavioral aversion to this compound

(A) Survival of *D. melanogaster* flies exposed to various concentrations of volatile AITC (no direct contact with the source of the AITC was allowed). The experimental arena (Figure Supplement 1A) consisted of two chambers, one housing a group of 8-10 flies and the other containing four 5 µL of AITC. All flies survived exposure to the solvent control and AITC 1:250 or 1:500 vol/vol. Flies exposed to higher concentrations of AITC survived less than 20 minutes, while those exposed to 1:5 or 1:2.5 vol/vol survived less than 10 minutes (**** $p<0.0001$, log-rank Mantel-Cox tests against the control). **(B)** Schematic and representative single sensillum recording (SSR) from pb1 OSNs upon stimulation with AITC 1:100 vol/vol. **(C)** SSR from all *D. melanogaster* antennae (ab) and palp (pb) basiconic sensilla to AITC stimulation (1:100 vol/vol). Here and thereafter, bar graph bars represent the control-subtracted net number of spikes (mean ± SEM) unless otherwise noted, and symbols indicate individual data points. AITC activates pb1a neurons the most, followed by ab4a neurons (n=6-10 recordings/sensilla type from 6 animals). **(D)** Responses from pb1 sensilla of Canton-S, w^{1118}, $TrpA1^{-}$, and *Or42a-/- D. melanogaster* flies to 1:100 vol/vol AITC stimulation. Flies from all genotypes except *Or42a-* responded to AITC, which indicates that *OR42a* is required for olfactory detection of this odor in pb1a (n=6-9 sensilla/genotype from 3-4 animals/genotype). Responses from all genotypes were different from those of *Or42a* mutants (Kruskal-Wallis ANOVA followed by Dunn's multiple comparisons, *$p<0.05$). **(E)** Food consumption of mutants and background genotype control flies in presence or absence of a non-toxic concentration of volatile AITC (1:500 vol/vol). Data represents the fly's normalized feeding scores (horizontal bars: median, edges of boxes: 25 and 25% quartiles, whiskers: 10 and 90% quartiles) in presence of AITC volatiles; the dashed line at 1 indicates neither aversion nor feeding enhancement. AITC volatiles strongly reduced feeding in control flies (median=0.35; one-sample signed rank test against median=1, $p<0.001$, n=16). AITC volatiles slightly

867 reduced feeding in *Or42a* mutants (median=0.83, p<0.05, n=14), but their normalized feeding score was
868 statistically different from that of control flies (Mann-Whitney U test, ***p<0.001, n=16, 14). **(F)**
869 Positional olfactory assay. Groups of 10-12 non-starved females were released in the middle of a
870 dispositive consisting of two glass tubes, each connected to a glass vial containing 10 µl of AITC 1:500
871 vol/vol or 10 µL of the solvent control (Figure supplement 1B). The number of flies in each of the glass
872 tubes were counted every five 5 minutes until minute 35, and then again at 65 minutes. Data show the %
873 of insects (mean ± SEM) in the tube closest to the odorant source at each timepoint (n=15/genotype).
874 The dotted line at 50% indicates random distribution between the two tubes. Control insects avoided the
875 tube closest to the odor source at 25, 30, 35 and 65 minutes (one-sample signed rank tests against
876 median=50%, ***p<0.005 in all cases; p=0.068 at 20 minutes). *Or42a-/-* mutants distributed randomly
877 between the two tubes at all timepoints (at 30 and 35 minutes p=0.055 and 0.078, respectively) except at
878 65 minutes (**p<0.01). **(G)** Positional olfactory assay using *Orco-/-* flies in which orco olfactory
879 function was specifically rescued in the OR42a circuit. Tests were conducted as in **F** using AITC 1:500
880 vol/vol. The two parental control lines (*UAS-Orco* and *Or42a-Gal4*) distributed at random between the
881 two tubes, while rescued flies (*Or42a-Gal4>UAS-Orco*) significantly avoided the tube closest to the
882 odor source from minute 15 onwards (*p<0.05; **p<0.01; ****p<0.001, n=15, 16, 13).

883

884 **Figure 2: Functional characterization of maxillary palp OSNs in *D. melanogaster* and *Scaptomyza***
885 **species.**

886 Single sensillum recordings (SSRs) were conducted from maxillary palp OSNs in *D. melanogaster*
887 (*Dmel*), *S. hsui* (*Shsu*), *S. pallida* (*Shsu*), *S. flava* (*Sfla*), and *S. montana* (*Smon*). Stimuli (all presented at
888 1:100 vol/vol) included diagnostic chemicals used to identify Ors in *D. melanogaster* such as ethyl
889 acetate (to identify Or42a in *Dmel* pb1a), 4-ethylguaiacol (Or71a in *Dmel* pb1b), fenchone (Or85e in
890 *Dmel* pb2a), guaiacol (Or46a in *Dmel* pb2b), and phenethyl acetate (Or85d in *Dmel* pb3b), along with
891 fruit volatiles, green leaf volatiles (GLVs), and Brassicales plant-derived isothiocyanate (ITCs). Each
892 panel depicts the control-subtracted net number of spikes/sec (average ± SEM, n=18-27 sensilla from 3-
893 4 animals/species) in response to odor stimulation (duration=1 sec). All sensilla housed two OSNs,
894 labeled "a" (darker color) and "b" (lighter color). Their response profiles and stereotyped locations
895 within the palp support the classification of *Scaptomyza* sensilla in three types (Figure 3, Supplementary
896 figure 5), named pb1-like, pb2-like, and pb3-like. In all *Scaptomyza* species we identified OSNs
897 exhibiting an odorant tuning pattern similar to that of *Dmel* pb1a sensilla. Among these, one OSN type

898 co-housed with pb1a-like OSNs exhibited a tuning pattern comparable to that of *Dmel* pb1b, while the
899 other OSN co-housed with pb1a-like OSNs showed subthreshold activity and thus it was excluded from
900 analysis. While pb1a sensilla from all species responded to AITC, pb1a-like from *S. flava* and *S.*
901 *montana* additionally responded to other ITC compounds. Mustard specialization occurred at the clade
902 leading to the common ancestor of these two species, denoted by the leaf cartoon. AITC: Allyl ITC,
903 IBITC: Isobutyl ITC, BITC: Butyl ITC, SBITC: Sec-butyl ITC, PITC: Phenethyl ITC.
904

905 **Figure 3: High expression of *Or42a* paralogs and over-representation of *Or42a*-positive-OSNs in**
906 **the maxillary palp of mustard specialist flies.**
907 **(A)** Picture of SSR from *Sfla* maxillary palp sensilla (top left) and a representative anatomical mapping
908 of *S. flava* palp sensilla (bottom left) obtained using diagnostic chemicals. Squares, triangles, and circles
909 in the cartoon indicate the location of the three types of maxillary palp *Sfla* sensilla, and bars in the
910 graph (right) represent the number of each sensilla type (green: pb1-like, red: pb2-like, purple: pb3-like)
911 in *Dmel* and the four *Scaptomyza* species (see Figure supplement 4 for individual maps; n=3
912 animals/species, symbols). Asterisks indicate significant differences in the number of pb sensilla within
913 a species (one-way ANOVA with Holm-Šídák's multiple comparisons test, **p<0.0001). **(B)** Schematic
914 of *Or42a* syntenic regions in the genomes of *Spal* and *Sfla*, with a gene triplication in the *Sfla* genome at
915 the syntenic region of *Spal Or42a2* (*Sfla Or42a2*, *Sfla Or42a3*, and *Sfla Or42a4*). **(C)** Maxillary palp
916 RNA seq of *Spal* and *Sfla Or*s (n=3 replicates/sex and species; symbols), indicating high expression of
917 *Spal Or42a2*, *Sfla Or42a2*, *Sfla Or42a3*, *Sfla Or42a4*, and the absence of *Or42a1* from *S. pallida* and *S.*
918 *flava*. *Or*s with the log2 (RPM +1) < 1 average values (n=3) were excluded. **(D-D")** Representative
919 images of HCR RNA FISH from the maxillary palps of *Spal* and *Sfla* showing *Or42a*-positive-OSNs (**D**,
920 green), *Orco*-positive-OSNs (**D'**, magenta**),** and the merged signals **(D'',** white indicates co-localization
921 of *Or42a*-positive-OSNs and *Orco*-positive-OSNs**)**. Scale bar: 20µm. **(E)** Number of *Or42a*-positive-
922 OSNs and *Orco*-positive-OSNs in one maxillary palp of *S. pallida* and *S. flava* (left panel) and ratio
923 between them (right panel). The number of both cell types as well as their percentage ratio was
924 significantly higher in *S. flava* (Mann-Whitney U tests, ** p<0.01 in both cases; n=5 animals/species).

925

926 **Figure 4: Functional characterization of chimeric Or42a (A181D and S301P) and Or42a from *D.***
927 ***melanogaster*, *S. pallida*, and *S. flava***

928 **(A)** Representative SSR from *Dmel* at1 sensilla OSNs expressing species-specific *Or42a* under the
929 control of *Or67d* ^{Gal4} (fly genotype: *UAS-Or42a; Or67d* ^{Gal4}) in response to BITC or γ-hexalactone
930 stimulation. Horizontal bars indicate the onset of the stimulus and its duration (1 sec). **(B)** Responses of
931 at1 OSNs (n=6-8 sensilla from 3-4 animals/genotype) expressing species-specific *Or42a* upon
932 stimulation with *trans*-2-hexenal (a general leaf odor released upon leaf mechanical damage such as
933 crushing), various ITCs produced by mustard plants (AITC, IBITC, BITC, SBITC), and γ-hexalactone,
934 which is produced by various fruits. All paralogs except *Sfla*Or42a2 responded to trans-2-hexenal. OSNs
935 expressing *Dmel* and *Spal* paralogs responded strongly to γ-hexalactone. OSNs expressing any of the
936 paralogs responded to AITC, but OSNs expressing *Sfla Or42a3* or *Or42a4* additionally responded to
937 other ITCs. **(C)** Schematic representation of chimeric Or42a with two amino acid substitutions (A181D
938 and S301P) in the background of *Sfla* Or42a3. Lateral view of the 3D structure of A181D, S301P
939 predicted by ColabFold (left) using PyMol2.5.3. *Sfla* Or42a3-derived amino acids are indicated in
940 magenta, and the substitutions with *Sfla* Or42a4-derived amino acids are represented in green. The upper
941 and lower sections represent the extracellular and the intracellular region, respectively (C: terminal C
942 section). The middle and right panels respectively display extracellular and lateral views of alignment of
943 the predicted structures of *Sfla* Or42a3, *Sfla* Or42a4, and the chimera. The extracellular region at S5 and
944 S6 (red arrows) highlight the local structural differences between *Sfla* Or42a3 and Or42a4 where the
945 A181D, S301P overlaps with the local structure of *Sfla* Or42a4. **(D-F)** Representative SSR from *Dmel*
946 at1 sensilla expressing heterologous *Sfla* Or42a3, Or42a4, and the chimera (genotypes of *UAS-*
947 *Or42a/CyO; Or67d* ^{Gal4}) upon stimulation with BITC or γ-hexalactone (**D**), population responses, with
948 green circles indicating responses to BITC and purple rectangles indicating responses to γ-hexalactone
949 (**E**, n=6-10 sensilla from 3-4 animals/genotype), and response ratio, where green represents *Sfla* Or42a3,
950 purple represents *Sfla* Or42a4, and blue represents A181D S307P (**F**, response to BITC stimulation/
951 response to BITC + response to γ-hexalactone). *p<0.01, Kruskal-Wallis ANOVA followed by Dunn's
952 multiple comparisons.
953

954 **FIGURE SUPPLEMENT CAPTIONS:**

955 **Figure supplement 1: Schematic representations of behavioral assays. (A)** Survival assay. Groups of
956 mated female flies (n=10) were placed in the upper chamber and monitored every 10 minutes in
957 presence of volatile chemicals (4 drops of a 5 µl solution in the lower chamber). The top and the bottom
958 chambers were separated by a fabric mesh, preventing direct contact between the flies and the chemical

959 solutions. **(B)** Feeding assay in presence of odors. Groups of 24 hours wet-starved mated female flies
960 (n=11-15) were transferred to a vial containing a piece of filter paper impregnated with 160 µl of 50 mM
961 D-glucose dyed blue. A small container affixed to the flug vial had a piece of filter paper loaded with 10
962 µl of an odorant solution or the solvent control, and because the opening was enclosed by mesh, flies
963 could smell but not contact the odor source. After 15 minutes, vials were frozen for at least 60 minutes,
964 the amount of blue dye in the abdomen of each fly in a vial was quantified blind to treatment, and a
965 feeding score was calculated for each vial as explained in materials and methods. **(C)** Positional
966 olfactory assay. Groups of 10-12 non-starved mated females were briefly cold anesthetized in a small
967 piece of clear Tygon tube, which was then used to connect the narrow ends of two cut glass Pasteur
968 pipettes. The distal end of each glass pipette was connected (via a piece of Tygon tube) to a 0.5 mL glass
969 vial containing 10 µL of the odor solution or the solvent control; a piece of fabric mesh prevented
970 insects from entering the vials containing the odor or control solutions. The number of flies in each of
971 the two tubes, as well as in the middle "release" section, were counted every five minutes until minute
972 35, and in tests with AITC, again at 65 minutes. The % of insects that choose one or the other tube over
973 the total number of insects released, and the % of insects in the tube closest to the odor source over the
974 total number of insects that choose one or the other tube, was then calculated for each time point.

975 **Figure supplement 2. γ-hexalactone does not affect fly survival and mediates olfactory attraction**
976 **via activation of Or42a in *D. melanogaster*. (A)** Feeding assay, as in Figure 1E, but using γ-
977 hexalactone (1:50 vol/vol). Flies were allowed to feed for 10 minutes, frozen, and scored blind to
978 treatment. Data were normalized (feeding in presence of the odor/feeding in absence of the odor) to
979 account for potential day-to-day and genotype variability. Normalized feeding of wild-type (Canton-S)
980 flies significantly increased in presence of volatile γ-hexalactone (one-sample signed rank test against
981 expected median=1, $p<0.001$, n=25), but this enhancement effect was lost in *Or42a-/-* mutants ($p>0.05$).
982 The horizontal dotted line at 1 indicates neither feeding aversion nor enhancement. **(B)** Percentage of
983 odor choice in the positional olfactory assay, as in Figure 1F, but using γ-hexalactone 1:10 vol/vol. The
984 number of flies in the tube closest to the odor source and in the tube closest to the solvent control was
985 counted every 5 minutes until minute 35. The dotted line at 50% indicates random distribution between
986 the two tubes. Control genotype flies significantly prefer the tube closest to the odor source at various
987 time points (*$p<0.05$, one-sample signed rank tests against median=50%; $p=0.074$ and $p=0.064$ at 15
988 and 25 minutes; n=19). *Or42a-/-* mutant flies were randomly distributed between the two tubes at all
989 time points ($p>0.05$ in all cases; n=19). **(C-D):** Percentage of flies that choose either tube in the

990 positional assay [(# of flies in one or the other tube / # of flies released) *100] in tests using AITC 1:500
991 vol/vol vs. m oil **(C)** or γ-hexalactone 1:10 vol/vol vs DMSO **(D)**. Similar proportions of genotype
992 control and *Or42a-/-* mutant flies choose one or the other tube at all time points in tests with AITC
993 (Mann-Whitney U tests, $p>0.05$ in all cases), but a significantly larger proportion of control flies choose
994 either tube in tests with γ-hexalactone (*$p<0.05$, ***$p<0.005$). (**E**) Survival assay, as in Figure 1A, but
995 using γ-hexalactone at various concentrations from 1/500 to 1/2.5 vol/vol. This odor had no effect on fly
996 mortality within at least 60 minutes. **(F)** SSR from all *D. melanogaster* antennae (ab) and palp basiconic
997 (pb) sensilla to stimulation with γ-hexalactone 1:100 vol/vol. Represented are the control-subtracted net
998 number of spikes and individual data points. Pb1a neurons are the most strongly activated by γ-
999 hexalactone, all other sensilla showed responses ≦20 spikes/second.

1000

1001 **Figure supplement 3: Hierarchical cluster analysis based on odorant response profiles across**
1002 **species. (A)** Hierarchical clusters were constructed using odorant response data from *Dmel, Shsu, Spal,*
1003 *Sfla,* and *Smon* using R studio v1.4.1717. A terminal node corresponds to a single recording from the
1004 individual sensilla. N=6-8 sensilla from 3-4 animals. **(B)** Hierarchical clusters were created for each
1005 sensilla type, including pb1-like, pb2-like, and pb3-like, using the odorant response (control-subtracted
1006 net number of spikes) average from each species as inputs. **(C)** The species phylogeny (left: Kim et al.,
1007 2021, eLife) and palp functional dendrogram (right) highlight the relevance of niche differences in
1008 shaping odorant responses. The palp functional dendrogram was generated using odorant response
1009 average for each species.

1010

1011 **Figure supplement 4. Location and percentages of the three different maxillary palp basiconic**
1012 **(pb) sensilla across species.** Classification of maxillary palp pb sensilla using SSRs and stimulation
1013 with diagnostic odorants. Data represents the proportion of pb1 and pb1-like (green), pb2 and pb2-like
1014 (red), and pb3 and pb3-like (magenta) in *Dmel, Shsu, Spal, Sfla,* and *Smon*. The total number of sensilla
1015 identified in each animal is indicated between parentheses. The schematic positions of pb sensilla in
1016 each of the three replicates (R1, R2, and R3) from each species are shown on the right. *Sfla* and *Smon*
1017 exhibited a larger number of pb1 compared to the microbe-feeder species, both in absolute numbers and
1018 proportions.

1019

1020 **Figure supplement 5: Maxillary palp and body area dimensions across species. (A)** A representative
1021 photograph and measurement of a male *Sfla* viewed under a conventional dissection microscope. The
1022 areas of the maxillary palp and of the body are respectively indicated by the broken magenta and green
1023 lines. Body size was defined as the sum of the head, thorax (excluding legs and wings) and abdomen
1024 areas. **(B)** Data (mean ± SEM, symbols indicate individual measurements, n=4 animals/species)
1025 represents the palp (top) and body size (middle) areas, along with their ratio (bottom) in *D.*
1026 *melanogaster, S. hsui, S. pallida*, and *S. flava*.

1027

1028 **Figure supplement 6: Or42a gene tree constructed by RAxML.** Maximum-likelihood gene tree with
1029 1000 bootstrap cycles using *Shsu Or42a1*, *Spal Or42a1*, *Sgra Or42a1*, *Smon Or42a1*, *Sfla Or42a1*, *Shsu*
1030 *Or42a2*, *SpalOr42a2*, *Sgra Or42a2*, *Sfla Or42a2*, *Smon Or42a*, *Sfla Or42a2*, *Sfla Or42a3*, *Sfla Or42a4*,
1031 and *Dmel Or42a* as an outgroup, generated by RAxML (v8.2.19) (Stamatakis 2014) after alignment by
1032 MAFFT v7 (Katoh and Standley 2013). Bootstrap values for the gene trees are denoted only when the
1033 values were smaller than 80. The tree was displayed by FigTree v1.4.3 (Rambaut 2009)
1034 **Figure Supplement 7: Maxillary palp RNA seq of *Spal* and *Sfla Or*s.** The heatmap displays
1035 Log2[RPM+1] values for *Or*s expression in the maxillary palps of *S. flava* and *S. pallida* across both
1036 sexes (n=3). Gray boxes indicate that the corresponding genes were unidentified in the genomes of the
1037 species.

1038

1039 **Figure Supplement 8: Dose-dependent responses of OSNs from *D. melanogaster* pb1a and**
1040 ***Scaptomyza* pb1a-like sensilla to stimulation with various odorant concentrations.** Responses of
1041 pb1a OSNs across species upon stimulation with various concentrations (ranging from 10^{-2} to 10^{-5}
1042 vol/vol) of γ-hexalactone, ethyl butyrate, trans-2-hexenal, AITC, IBITC, BITC, and SBITC (6-8 sensilla
1043 from n=3-4 animals/species). The chemical structures of each compound are shown on the left. Half
1044 maximal effective concentrations (EC_{50}) are shown for each chemical and species. IBITC, BITC, and
1045 SBITC were only tested in *Sfla* and *Smon* pb1a, as BITC at 10^{-2} vol/vol failed to activate OSNs in pb1a
1046 from microbe-feeding species (Figure 2A). The EC_{50} values for γ-hexalactone were consistently lower in
1047 microbe-feeding species compared to Brassicales specialists, suggesting a lower sensitivity in the non-
1048 specialist microbivores. *S. flava* exhibited a lower EC_{50} value for *trans*-2-hexenal compared to *S.*
1049 *montana* and the other microbivorous species. This heightened sensitivity to a general leaf odor in *S.*

1050 *flava* aligns with its potentially broader host range than *S. montana*, as it can be reared on plants from
1051 other families, such as Fabaceae or Caryophyllaceae (Martin 2004), rather than being strictly limited to
1052 Brassicales.
1053

1054 **Figure supplement 9: Screening of candidate amino acids using branch-site test following**
1055 **ColabFold 3D prediction. (A)** Alignment of amino acids of *Spal* Or42a2, *Sfla* Or42a3, and *Sfla*
1056 Or42a4, and the A181D S301P chimera. Red arrowheads denote the sites where site-directed-
1057 mutagenesis was performed to generate the A181D, S301P chimera. **(B)** Lateral view of alignment of
1058 3D predictions of *Sfla* Or42a3, *Sfla* Or42a4, and the chimera using ColabFold and PyMol 2.5.3. Red
1059 rectangles highlight the sites of local structural variance between *Sfla* Or42a3 and Or42a4. The A181D,
1060 S301P chimera shows a closer alignment with Or42a4. S5' and S6' are enlarged views of S5 and S6,
1061 respectively.

1062 **Figure supplement 10: Responses of OSNs expressing homozygous Or42a to stimulation with**
1063 **BITC and γ-hexalactone.** Left: responses of OSNs expressing homozygous *Sfla* Or42a3, *Sfla* Or42a4,
1064 or A181D S307P (*UAS-Or42a; Or67d* ^{Gal4}) to stimulation with BITC and γ-hexalactone (left; n=16-30
1065 from 5-10 animals). Right: ratio between responses to BITC and the sum of the responses evoked by
1066 stimulation with BITC and γ-hexalactone. In these homozygous flies, increased BITC sensitivity or
1067 decrease γ-hexalactone sensitivity (Figure 4) was not observed, indicating that while two amino acids
1068 substitutions (A181D S307P) can change the ligand specificity (Figure 4), additional amino acids are
1069 necessary for achieving further robustness in this ligand switch. Kruskal-Wallis test with Dunn's
1070 multiple comparisons, *$p<0.05$ between *Sfla* Or42a4 and A181D S301P.

1071

1072 **SUPPLEMENTARY MATERIAL AND METHODS:**

1073 **Measurement of maxillary palps and body size**
1074 Two-to-ten-day old male *Dmel, Shsu, Spal,* and *Sfla* flies with their heads facing up and their bodies
1075 sideway were mounted and imaged using a commercial camera under a conventional microscope. The
1076 areas of the maxillary palps and the body (head, thorax excluding legs and wings, and abdomen) were
1077 measured using ImageJ v1.54.

1078 **Dilution series**

1079 *trans*-2-hexenal, AITC, IBITC, SBITC, and ethyl butyrate were diluted in mineral oil, and γ-hexalactone
1080 was diluted in DMSO to 10^{-5} to 10^{-2} vol/vol. Half maximal effective concentration (EC50) was
1081 generated by GraphPad Prism v10.2.1.

1082 **Construction of Or42a gene tree**

1083 Amino acid sequences of *Dmel Or42a,* and *Sfla Or42a1, Sfla Or42a2, Sfla Or42a3,* and *Sfla Or42a4*
1084 were obtained from Flybase (2024_01), and Goldman-Huertas et al., 2015. Blast searches were
1085 conducted to annotate *Shsu Or42a1, Spal Or42a1, Sgra Or42a1, Smon Or42a1, Sfla Or42a1, Shsu*
1086 *Or42a2, Spal Or42a2, Sgra Or42a2,* and *Smon Or42a2*, using *Sfla Or42a1* and *Sfla Or42a2* as query
1087 against the genomes of *S. hsui* (ASM1815282v1), *S. pallida* (ASM1815296v1), *S. graminum*
1088 (ASM1890183v1), and *S. montana* (ASM1890430v1). Amino acid sequences of *Shsu Or42a1, Spal*
1089 *Or42a1, Sgra Or42a1, Smon Or42a1, Sfla Or42a1, Shsu Or42a2, SpalOr4* (Katoh and Standley
1090 2013)*2a2, Sgra Or42a2, Sfla Or42a2, Smon Or42a, Sfla Or42a2, Sfla Or42a3, Sfla Or42a4,* and *Dmel*
1091 *Or42a* were aligned by MAFFT v7.511 with JTT as scoring matrix for amino acid sequences with L-
1092 INS-i strategy. Maximum-likelihood gene tree with 1000 bootstrap cycles using the above sequences
1093 were constructed with RAxML (v8.2.19)(Stamatakis 2014). GAMMA model of rate heterogeneity was
1094 applied. CDS and alignment of *Or42a* are included in Supplementary files 12 and 13, respectively.

1095 **SUPPLEMENTARY FILES:**

1096 Supplementary file 1: Chemical list

1097 Supplementary file 2: Control-subtracted net number of spikes/sec obtained from SSRs

1098 Supplementary file 3: Survival assay data

1099 Supplementary file 4: Consumption assay data

1100 Supplementary file 5: Olfactory positional assay data

1101 Supplementary file 6: Expression intensity from maxillary palp RNA-seq

1102 Supplementary file 7: OSNs counts of RNA FISH

1103 Supplementary file 8: Primer list

1104 Supplementary file 9: AlphaFold2 (Colabfold) prediction in pdb format

1105 Supplementary file 10: Pb sensilla counts by SSR

1106 Supplementary file 11: Measurements of maxillary palp and body areas

1107 Supplementary file 12: CDS of *Or42a* homologs in fasta format

1108 Supplementary file 13: Alignment of *Or42a* homologs in fasta format

1109

1110 **REFERENCES:**

1111

1112 Aguilar JM, Gloss AD, Suzuki HC, Verster KI, Singhal M, Hoff J, Grebenok R, Nabity PD, Behmer ST,
1113 Whiteman NK. 2024. Insights into the evolution of herbivory from a leaf‐mining fly.
1114 *Ecosphere* [Internet] 15. Available from:
1115 https://esajournals.onlinelibrary.wiley.com/doi/10.1002/ecs2.4764

1116 Ahuja I, Rohloff J, Bones AM. 2010. Defence mechanisms of Brassicaceae: implications for plant-insect
1117 interactions and potential for integrated pest management. A review. *Agron. Sustain. Dev.*
1118 30:311–348.

1119 Al-Anzi B, Tracey WD Jr, Benzer S. 2006. Response of Drosophila to wasabi is mediated by painless,
1120 the fly homolog of mammalian TRPA1/ANKTM1. *Curr. Biol.* 16:1034–1040.

1121 Ali JG, Agrawal AA. 2012. Specialist versus generalist insect herbivores and plant defense. *Trends*
1122 *Plant Sci.* 17:293–302.

1123 Anders S, Pyl PT, Huber W. 2015. HTSeq--a Python framework to work with high-throughput
1124 sequencing data. *Bioinformatics* 31:166–169.

1125 Auer TO, Khallaf MA, Silbering AF, Zappia G, Ellis K, Álvarez-Ocaña R, Arguello JR, Hansson BS,
1126 Jefferis GSXE, Caron SJC, et al. 2020. Olfactory receptor and circuit evolution promote host
1127 specialization. *Nature* 579:402–408.

1128 Becher PG, Bengtsson M, Hansson BS, Witzgall P. 2010. Flying the fly: long-range flight behavior of
1129 Drosophila melanogaster to attractive odors. *J. Chem. Ecol.* 36:599–607.

1130 Bell L, Oloyede OO, Lignou S, Wagstaff C, Methven L. 2018. Taste and flavor perceptions of
1131 glucosinolates, isothiocyanates, and related compounds. *Mol. Nutr. Food Res.* 62:e1700990.

1132 Benton R, Himmel NJ. 2023. Structural screens identify candidate human homologs of insect
1133 chemoreceptors and cryptic Drosophila gustatory receptor-like proteins. *Elife* 12:e85537.

1134 Benton R, Vannice KS, Gomez-Diaz C, Vosshall LB. 2009. Variant ionotropic glutamate receptors as
1135 chemosensory receptors in Drosophila. *Cell* 136:149–162.

1136 Bernays E, Chapman R. 1987. The evolution of deterrent responses in plant-feeding insects. In:
1137 Proceedings in Life Sciences. New York, NY: Springer New York. p. 159–173.

1138 Bernays E, Graham M. 1988. On the evolution of host specificity in phytophagous arthropods. *Ecology*
1139 69:886–892.

1140 Bischof J, Maeda RK, Hediger M, Karch F, Basler K. 2007. An optimized transgenesis system for
1141 Drosophila using germ-line-specific phiC31 integrases. *Proc. Natl. Acad. Sci. U. S. A.* 104:3312–
1142 3317.

1143 de Bruyne M, Clyne PJ, Carlson JR. 1999. Odor coding in a model olfactory organ: the Drosophila
1144 maxillary palp. *J. Neurosci.* 19:4520–4532.

1145 Butterwick JA, Del Mármol J, Kim KH, Kahlson MA, Rogow JA, Walz T, Ruta V. 2018. Cryo-EM
1146 structure of the insect olfactory receptor Orco. *Nature* 560:447–452.

1147 Carraher C, Dalziel J, Jordan MD, Christie DL, Newcomb RD, Kralicek AV. 2015. Towards an
1148 understanding of the structural basis for insect olfaction by odorant receptors. *Insect Biochem.*
1149 *Mol. Biol.* 66:31–41.

1150 Chen S, Zhou Y, Chen Y, Gu J. 2018. fastp: an ultra-fast all-in-one FASTQ preprocessor.
1151 *Bioinformatics* 34:i884–i890.

1152 Chen Y-CD, Dahanukar A. 2020. Recent advances in the genetic basis of taste detection in Drosophila.
1153 *Cell. Mol. Life Sci.* 77:1087–1101.

1154 Couto A, Alenius M, Dickson BJ. 2005. Molecular, anatomical, and functional organization of the
1155 Drosophila olfactory system. *Curr. Biol.* 15:1535–1547.

1156 Crowley-Gall A, Date P, Han C, Rhodes N, Andolfatto P, Layne JE, Rollmann SM. 2016. Population
1157 differences in olfaction accompany host shift in Drosophila mojavensis. *Proc. Biol. Sci.*
1158 [Internet] 283. Available from: https://www.ncbi.nlm.nih.gov/pmc/articles/PMC5013806/

1159 Cuellar-Nuñez ML, Luzardo-Ocampo I, Lee-Martínez S, Larrauri-Rodríguez M, Zaldívar-Lelo de
1160 Larrea G, Pérez-Serrano RM, Camacho-Calderón N. 2022. Isothiocyanate-Rich Extracts from
1161 Cauliflower (Brassica oleracea Var. Botrytis) and Radish (Raphanus sativus) Inhibited Metabolic
1162 Activity and Induced ROS in Selected Human HCT116 and HT-29 Colorectal Cancer Cells. *Int.*
1163 *J. Environ. Res. Public Health* [Internet] 19. Available from:
1164 http://dx.doi.org/10.3390/ijerph192214919

1165 Dekker T, Ibba I, Siju KP, Stensmyr MC, Hansson BS. 2006. Olfactory shifts parallel superspecialism
1166 for toxic fruit in Drosophila melanogaster sibling, D. sechellia. *Curr. Biol.* 16:101–109.

1167 Del Mármol J, Yedlin MA, Ruta V. 2021. The structural basis of odorant recognition in insect olfactory
1168 receptors. *Nature* 597:126–131.

1169 Dobin A, Davis CA, Schlesinger F, Drenkow J, Zaleski C, Jha S, Batut P, Chaisson M, Gingeras TR.
1170 2013. STAR: ultrafast universal RNA-seq aligner. *Bioinformatics* 29:15–21.

1171 Dobler S, Dalla S, Wagschal V, Agrawal AA. 2012. Community-wide convergent evolution in insect
1172 adaptation to toxic cardenolides by substitutions in the Na,K-ATPase. *Proc. Natl. Acad. Sci. U.*
1173 *S. A.* 109:13040–13045.

1174 Dweck HK, Ebrahim SA, Khallaf MA, Koenig C, Farhan A, Stieber R, Weißflog J, Svatoš A, Grosse-
1175 Wilde E, Knaden M, et al. 2016. Olfactory channels associated with the Drosophila maxillary
1176 palp mediate short- and long-range attraction. *Elife* [Internet] 5. Available from:
1177 https://www.ncbi.nlm.nih.gov/pmc/articles/PMC4927298/

1178 Dweck HKM, Carlson JR. 2020. Molecular logic and evolution of bitter taste in Drosophila. *Curr. Biol.*
1179 30:17-30.e3.

1180 Gloss A, Nelson Dittrich AC, Lapoint R, Goldman-Huertas B, Verster KI, Pelaez JL, Nelson AD,
1181 Aguilar JM, Armstrong E, Charboneau JLM, et al. 2019. Evolution of herbivory remodels a
1182 Drosophila genome. *bioRxiv* [Internet]. Available from:
1183 https://www.biorxiv.org/content/10.1101/767160v1

1184 Gloss AD, Vassão DG, Hailey AL, Nelson Dittrich AC, Schramm K, Reichelt M, Rast TJ, Weichsel A,
1185 Cravens MG, Gershenzon J, et al. 2014. Evolution in an ancient detoxification pathway is
1186 coupled with a transition to herbivory in the drosophilidae. *Mol. Biol. Evol.* 31:2441–2456.

1187 Goldman-Huertas B, Mitchell RF, Lapoint RT, Faucher CP, Hildebrand JG, Whiteman NK. 2015.
1188 Evolution of herbivory in Drosophilidae linked to loss of behaviors, antennal responses, odorant
1189 receptors, and ancestral diet. *Proceedings of the National Academy of Sciences* 112:3026–3031.

1190 Gonzalez F, Witzgall P, Walker WB. 2016. Protocol for heterologous expression of insect odourant
1191 receptors in Drosophila. *Front. Ecol. Evol.* [Internet] 4. Available from:
1192 https://www.frontiersin.org/journals/ecology-and-
1193 evolution/articles/10.3389/fevo.2016.00024/full

1194 Hashimoto Y, Yoshimura M, Huang R-N. 2019. Wasabi versus red imported fire ants: preliminary test
1195 of repellency of microencapsulated allyl isothiocyanate against Solenopsis invicta
1196 (Hymenoptera: Formicidae) using bait traps in Taiwan. *Appl. Entomol. Zool. (Jpn.)* 54:193–196.

1197 Haverkamp A, Hansson BS, Knaden M. 2018. Combinatorial codes and labeled lines: How insects use
1198 olfactory cues to find and judge food, mates, and oviposition sites in complex environments.
1199 *Front. Physiol.* 9:49.

1200 Himmel NJ, Moi D, Benton R. 2023. Remote homolog detection places insect chemoreceptors in a
1201 cryptic protein superfamily spanning the tree of life. *Curr. Biol.* 33:5023-5033.e4.

1202 Hopkins RJ, van Dam NM, van Loon JJA. 2009. Role of glucosinolates in insect-plant relationships and
1203 multitrophic interactions. *Annu. Rev. Entomol.* 54:57–83.

1204 Humphrey PT, Gloss AD, Alexandre NM, Villalobos MM, Fremgen MR, Groen SC, Meihls LN, Jander
1205 G, Whiteman NK. 2016. Aversion and attraction to harmful plant secondary compounds jointly
1206 shape the foraging ecology of a specialist herbivore. *Ecol. Evol.* 6:3256–3268.

1207 Ibanez S, Gallet C, Després L. 2012. Plant insecticidal toxins in ecological networks. *Toxins (Basel)*
1208 4:228–243.

1209 Jumper J, Evans R, Pritzel A, Green T, Figurnov M, Ronneberger O, Tunyasuvunakool K, Bates R,
1210 Žídek A, Potapenko A, et al. 2021. Highly accurate protein structure prediction with AlphaFold.
1211 *Nature* 596:583–589.

1212 Kang K, Pulver SR, Panzano VC, Chang EC, Griffith LC, Theobald DL, Garrity PA. 2010. Analysis of
1213 Drosophila TRPA1 reveals an ancient origin for human chemical nociception. *Nature* 464:597–
1214 600.

1215 Karageorgi M, Groen SC, Sumbul F, Pelaez JN, Verster KI, Aguilar JM, Hastings AP, Bernstein SL,
1216 Matsunaga T, Astourian M, et al. 2019. Genome editing retraces the evolution of toxin resistance
1217 in the monarch butterfly. *Nature* 574:409–412.

1218 Katoh K, Standley DM. 2013. MAFFT multiple sequence alignment software version 7: improvements
1219 in performance and usability. *Mol. Biol. Evol.* 30:772–780.

1220 Kim BY, Wang JR, Miller DE, Barmina O, Delaney E, Thompson A, Comeault AA, Peede D,
1221 D'Agostino ERR, Pelaez J, et al. 2021. Highly contiguous assemblies of 101 drosophilid
1222 genomes. *Elife* [Internet] 10. Available from: https://pubmed.ncbi.nlm.nih.gov/34279216/

1223 Kim SH, Lee Y, Akitake B, Woodward OM, Guggino WB, Montell C. 2010. *Drosophila* TRPA1
1224 channel mediates chemical avoidance in gustatory receptor neurons. *Proceedings of the National*
1225 *Academy of Sciences* 107:8440–8445.

1226 Kreher SA, Mathew D, Kim J, Carlson JR. 2008. Translation of sensory input into behavioral output via
1227 an olfactory system. *Neuron* 59:110–124.

1228 Kurtovic A, Widmer A, Dickson BJ. 2007. A single class of olfactory neurons mediates behavioural
1229 responses to a Drosophila sex pheromone. *Nature* 446:542–546.

1230 Lichtenstein EP, Morgan DG, Mueller CH. 1964. Insecticides in Nature, Naturally Occurring
1231 Insecticides in Cruciferous Crops. *J. Agric. Food Chem.* 12:158–161.

1232 Linz J, Baschwitz A, Strutz A, Dweck HKM, Sachse S, Hansson BS, Stensmyr MC. 2013. Host plant-
1233 driven sensory specialization in Drosophila erecta. *Proc. Biol. Sci.* 280:20130626.

1234 Liu X-L, Zhang J, Yan Q, Miao C-L, Han W-K, Hou W, Yang K, Hansson BS, Peng Y-C, Guo J-M, et
1235 al. 2020. The molecular basis of host selection in a Crucifer-specialized moth. *Curr. Biol.*
1236 30:4476-4482.e5.

1237 Maca, J., 1972. Czechoslovak species of the genus Scaptomyza Hardy (Diptera,Drosophilidae) and their
1238 bionomics. *Acta Entomologica Bohemoslovaca* 69, 119‑132

1239 MacLeod AJ, MacLeod G, Reader G. 1989. Evidence for the occurrence of butyl- and
1240 isobutylglucosinolates in seeds of Brassica oleracea. *Phytochemistry* 28:1405–1407.

1241 Mandel SJ, Shoaf ML, Braco JT, Silver WL, Johnson EC. 2018. Behavioral aversion to AITC requires
1242 both painless and dTRPA1 in Drosophila. *Front. Neural Circuits* 12:45.

1243 Mantel N. 1966. Evaluation of survival data and two new rank order statistics arising in its
1244 consideration. *Cancer Chemother. Rep.* 50:163–170.

1245 Martin NA. 2004. History of an invader,Scaptomyza flava(fallen, 1823) (Diptera: Drosophilidae). *N. Z.*
1246 *J. Zool.* 31:27–32.

1247 Matsunaga T, Reisenman CE, Goldman-Huertas B, Brand P, Miao K, Suzuki HC, Verster KI, Ramírez
1248 SR, Whiteman NK. 2021. Evolution of Olfactory Receptors Tuned to Mustard Oils in
1249 Herbivorous Drosophilidae. *Mol. Biol. Evol.* 39:msab362.

1250 Mirdita M, Schütze K, Moriwaki Y, Heo L, Ovchinnikov S, Steinegger M. 2022. ColabFold: making
1251 protein folding accessible to all. *Nat. Methods* 19:679–682.

1252 Mithöfer A, Boland W. 2012. Plant defense against herbivores: chemical aspects. *Annu. Rev. Plant Biol.*
1253 63:431–450.

1254 Mohamed AAM, Retzke T, Das Chakraborty S, Fabian B, Hansson BS, Knaden M, Sachse S. 2019.
1255 Odor mixtures of opposing valence unveil inter-glomerular crosstalk in the Drosophila antennal
1256 lobe. *Nat. Commun.* 10:1201.

1257 Noge K, Becerra JX. 2015. 4-Oxo-(E)-2-hexenal produced by Heteroptera induces permanent
1258 locomotive impairment in crickets that correlates with free thiol depletion. *FEBS Open Bio*
1259 5:319–324.

1260 Orre GUS, Wratten SD, Jonsson M, Hale RJ. 2010. Effects of an herbivore-induced plant volatile on
1261 arthropods from three trophic levels in brassicas. *Biol. Control* 53:62–67.

1262 Peláez JN, Gloss AD, Goldman-Huertas B, Kim B, Lapoint RT, Pimentel-Solorio G, Verster KI, Aguilar
1263 JM, Nelson Dittrich AC, Singhal M, et al. 2023. Evolution of chemosensory and detoxification
1264 gene families across herbivorous Drosophilidae. *G3* [Internet] 13. Available from:
1265 http://dx.doi.org/10.1093/g3journal/jkad133

1266 Peláez JN, Gloss AD, Ray JF, Chaturvedi S, Haji D, Charboneau JLM, Verster KI, Whiteman NK.
1267 2022. Evolution and genomic basis of the plant-penetrating ovipositor: a key morphological trait
1268 in herbivorous Drosophilidae. *Proc. Biol. Sci.* 289:20221938.

1269 Rambaut A. 2009. FigTree, version 1.4.3. *Computer program distributed by the author, website:*
1270 *http://tree.bio.ed.ac.uk/software/figtree/[accessed January 4, 2011]* [Internet]. Available from:
1271 https://scholar.google.com/citations?view_op=view_citation&hl=en&citation_for_view=JiYPDf
1272 oAAAAJ:W5xh706n7nkC

1273 Ray A, van der Goes van Naters W, Carlson JR. 2008. A regulatory code for neuron-specific odor
1274 receptor expression. *PLoS Biol.* 6:e125.

1275 Reichstein T, von Euw J, Parsons JA, Rothschild M. 1968. Heart poisons in the monarch butterfly. Some
1276 aposematic butterflies obtain protection from cardenolides present in their food plants. *Science*
1277 161:861–866.

1278 Reisenman CE, Scott K. 2019. Food-derived volatiles enhance consumption in Drosophila
1279 melanogaster. *J. Exp. Biol.* 222:jeb202762.

1280 Scott K. 2018. Gustatory processing in Drosophila melanogaster. *Annu. Rev. Entomol.* 63:15–30.

1281 Semmelhack JL, Wang JW. 2009. Select Drosophila glomeruli mediate innate olfactory attraction and
1282 aversion. *Nature* 459:218–223.

1283 Shiraiwa T. 2008. Multimodal chemosensory integration through the maxillary palp in Drosophila. *PLoS*
1284 *One* 3:e2191.

1285 Southwood T. 1972. insect/plant relationship--an evolutionary perspective. Available from:
1286 https://www.semanticscholar.org/paper/insect%2Fplant-relationship--an-evolutionary-
1287 Southwood/635ed400c02b62dca75e90d7ee3e664383d480be

1288 Stamatakis A. 2014. RAxML version 8: a tool for phylogenetic analysis and post-analysis of large
1289 phylogenies. *Bioinformatics* 30:1312–1313.

1290 Stensmyr MC, Dweck HKM, Farhan A, Ibba I, Strutz A, Mukunda L, Linz J, Grabe V, Steck K,
1291 Lavista-Llanos S, et al. 2012. A conserved dedicated olfactory circuit for detecting harmful
1292 microbes in Drosophila. *Cell* 151:1345–1357.

1293 Takagi S, Sancer G, Abuin L, Stupski SD, Roman Arguello J, Prieto-Godino LL, Stern DL, Cruchet S,
1294 Álvarez-Ocaña R, Wienecke CFR, et al. 2024. Olfactory sensory neuron population expansions
1295 influence projection neuron adaptation and enhance odour tracking. *Nat. Commun.* 15:7041.

1296 Tocmo R, Veenstra JP, Huang Y, Johnson JJ. 2021. Covalent modification of proteins by plant-derived
1297 natural products: Proteomic approaches and biological impacts. *Proteomics* 21:e1900386.

1298 Whiteman NK, Gloss AD, Sackton TB, Groen SC, Humphrey PT, Lapoint RT, Sønderby IE, Halkier
1299 BA, Kocks C, Ausubel FM, et al. 2012. Genes involved in the evolution of herbivory by a leaf-
1300 mining, Drosophilid fly. *Genome Biol. Evol.* 4:900–916.

1301 Whiteman NK, Groen SC, Chevasco D, Bear A, Beckwith N, Gregory TR, Denoux C, Mammarella N,
1302 Ausubel FM, Pierce NE. 2011. Mining the plant-herbivore interface with a leafmining
1303 Drosophila of Arabidopsis. *Mol. Ecol.* 20:995–1014.

1304 Winde I, Wittstock U. 2011. Insect herbivore counteradaptations to the plant glucosinolate-myrosinase
1305 system. *Phytochemistry* 72:1566–1575.

1306 Wu X, Huang H, Childs H, Wu Y, Yu L, Pehrsson PR. 2021. Glucosinolates in Brassica vegetables:
1307 Characterization and factors that influence distribution, content, and intake. *Annu. Rev. Food Sci.*
1308 *Technol.* 12:485–511.

1309 Zhao J, Chen AQ, Ryu J, Del Mármol J. 2024. Structural basis of odor sensing by insect heteromeric
1310 odorant receptors. *Science* 384:1460–1467.

1311 Zimmermann C, Dähn S, Wagner AE. 2024. Effect of allyl-isothiocyanate on survival and antimicrobial
1312 peptide expression following oral bacterial infections in Drosophila melanogaster. *Front.*
1313 *Immunol.* 15:1404086.

Figure 1

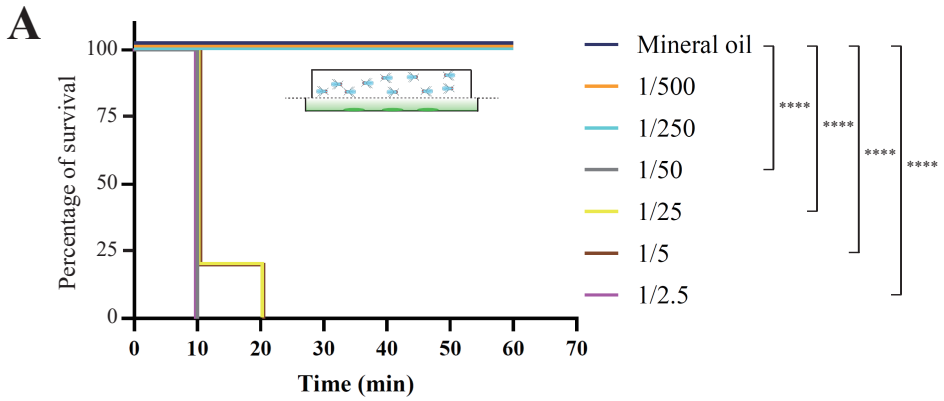
A
Percentage of survival
Time (min)
Mineral oil
1/500
1/250
1/50
1/25
1/5
1/2.5
****

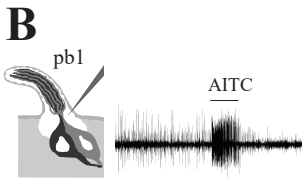
B
pb1
AITC

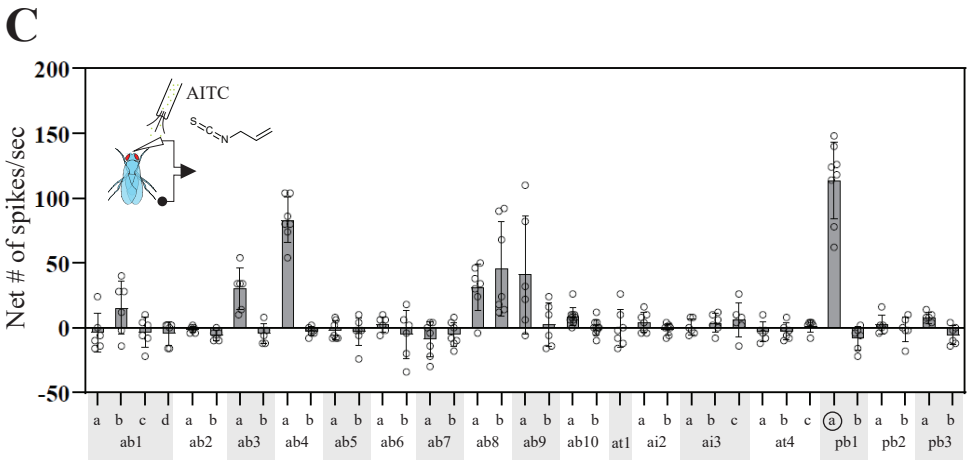
C
AITC
Net # of spikes/sec
ab1
ab2
ab3
ab4
ab5
ab6
ab7
ab8
ab9
ab10
at1
ai2
ai3
at4
pb1
pb2
pb3

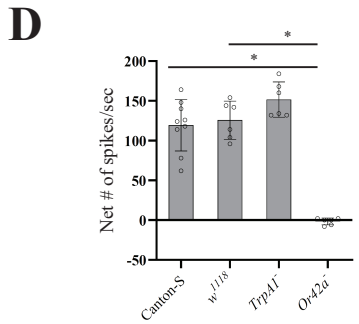
D
Net # of spikes/sec
Canton-S
w1118
TrpA1-
Or42a-

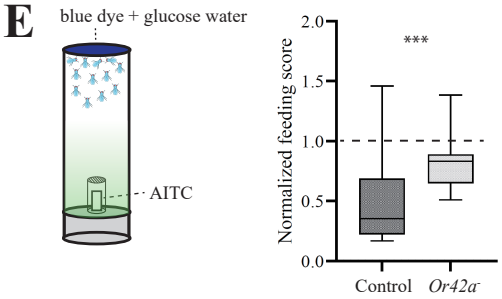
E
blue dye + glucose water
AITC
Normalized feeding score
Control
Or42a-
***

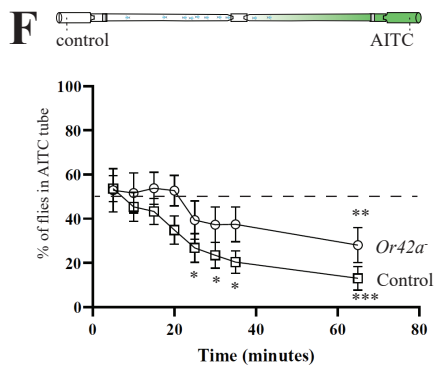
F
control
AITC
% of flies in AITC tube
Or42a-
Control
Time (minutes)

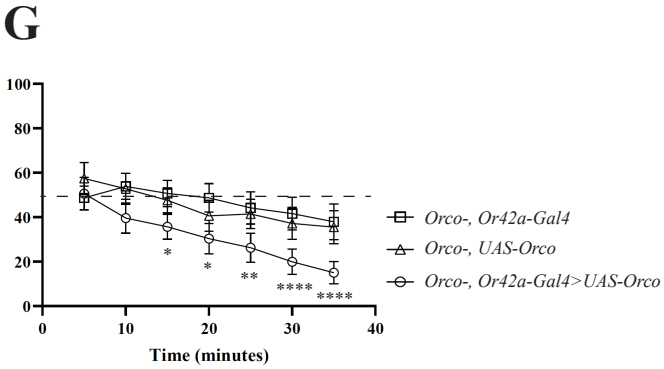
G
Orco-, Or42a-Gal4
Orco-, UAS-Orco
Orco-, Or42a-Gal4>UAS-Orco
Time (minutes)

Figure 2

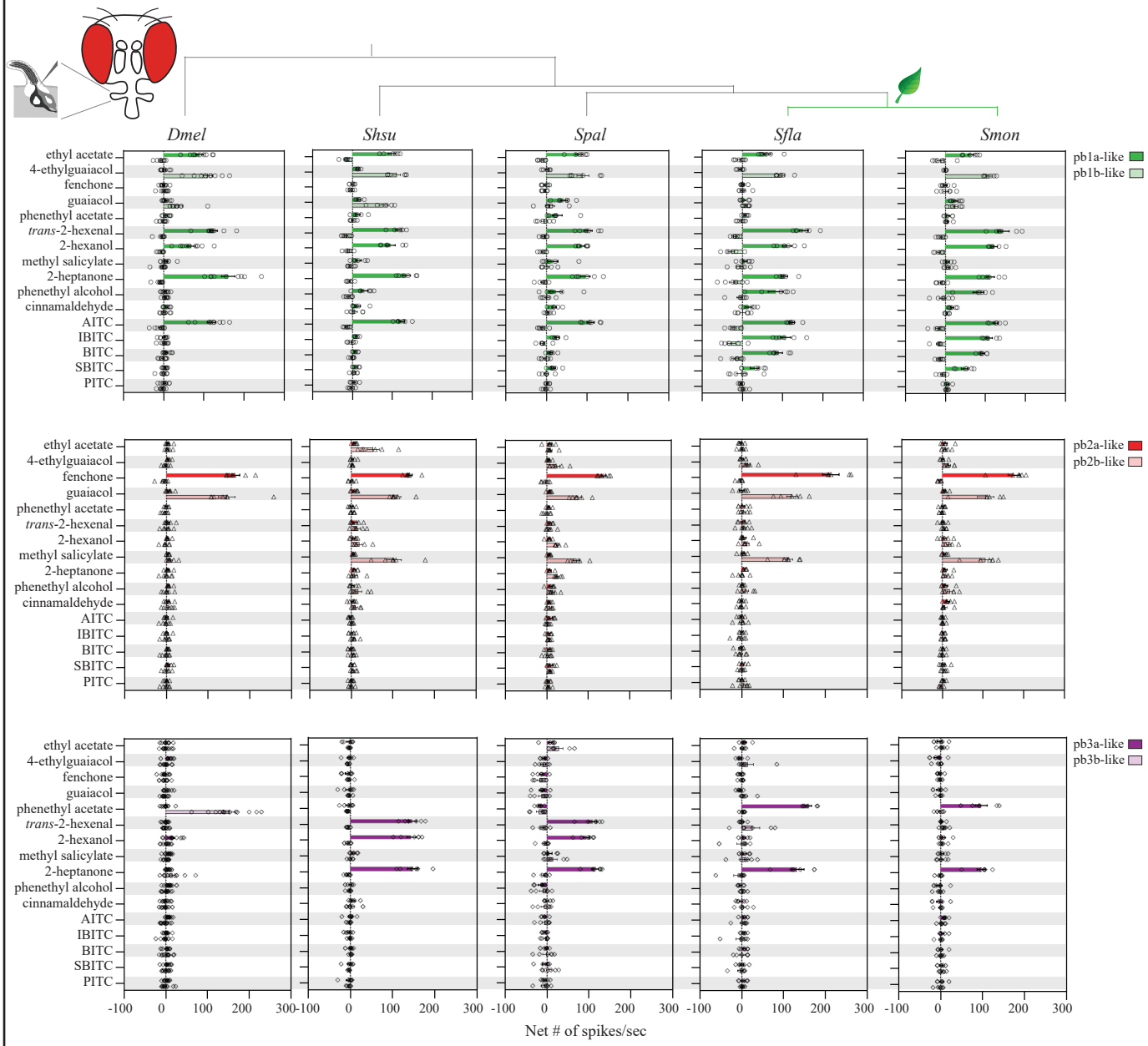
Dmel
Shsu
Spal
Sfla
Smon
ethyl acetate
4-ethylguaiacol
fenchone
guaiacol
phenethyl acetate
trans-2-hexenal
2-hexanol
methyl salicylate
2-heptanone
phenethyl alcohol
cinnamaldehyde
AITC
IBITC
BITC
SBITC
PITC
pb1a-like
pb1b-like
pb2a-like
pb2b-like
pb3a-like
pb3b-like
-100
0
100
200
300
Net # of spikes/sec

Figure 3

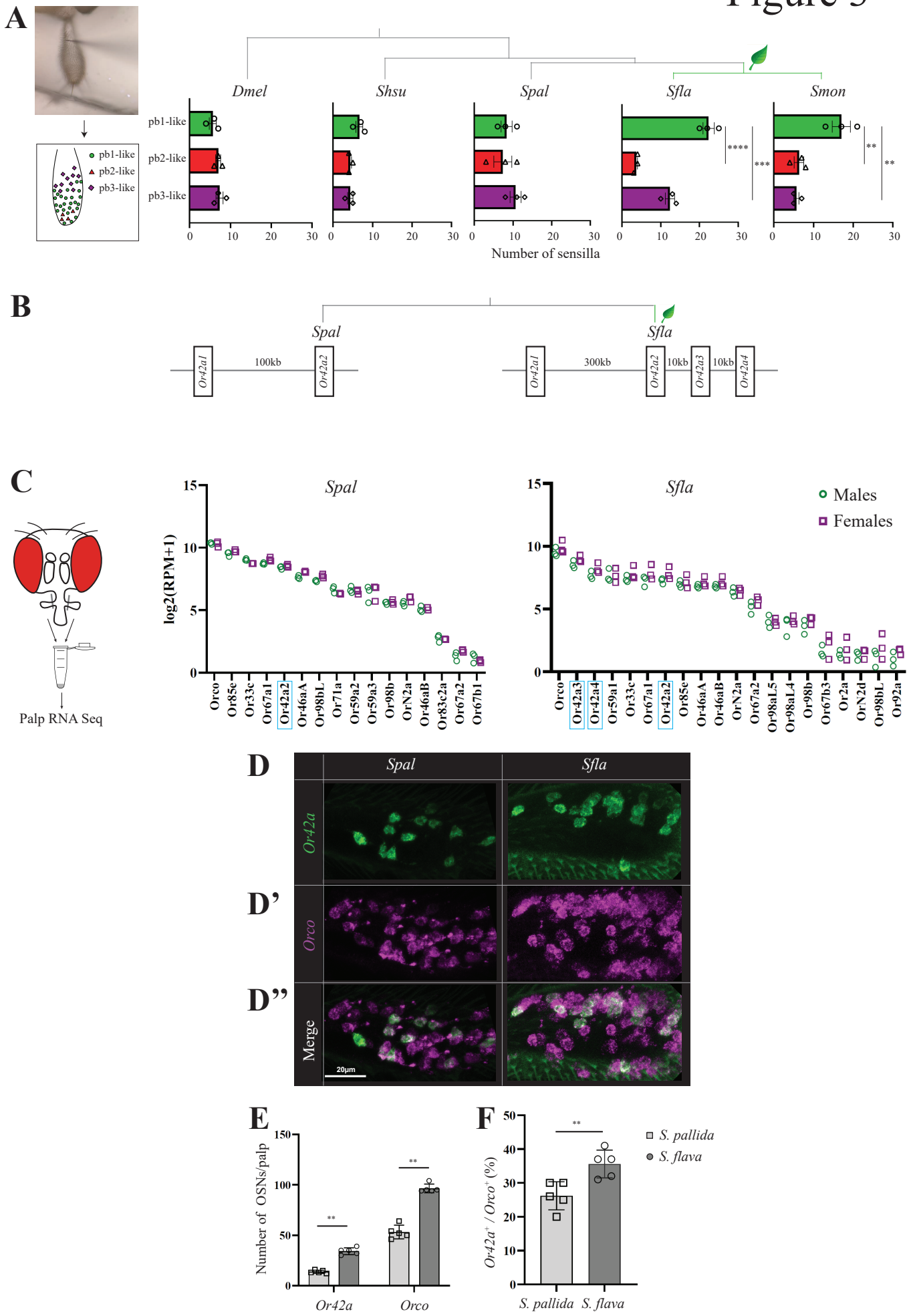
A
pb1-like
pb2-like
pb3-like
Dmel
Shsu
Spal
Sfla
Smon
Number of sensilla
B
Spal
Sfla
Or42a1
100kb
Or42a2
300kb
10kb
Or42a3
Or42a4
C
Palp RNA Seq
log2(RPM+1)
Males
Females
Orco
Or85e
Or33c
Or67a1
Or42a2
Or46aA
Or98bL
Or71a
Or59a2
Or59a3
Or98b
OrN2a
Or46aB
Or83c2a
Or67a2
Or67b1
Or42a3
Or42a4
Or59a1
Or85c
Or46aA
Or46aB
OrN2a
Or67a2
Or98aL5
Or98aL4
Or98b
Or67b3
Or2a
OrN2d
Or98bL
Or92a
D
D'
D''
Or42a
Orco
Merge
20μm
E
Number of OSNs/palp
Or42a
Orco
F
Or42a+ / Orco+ (%)
S. pallida
S. flava

Figure 4

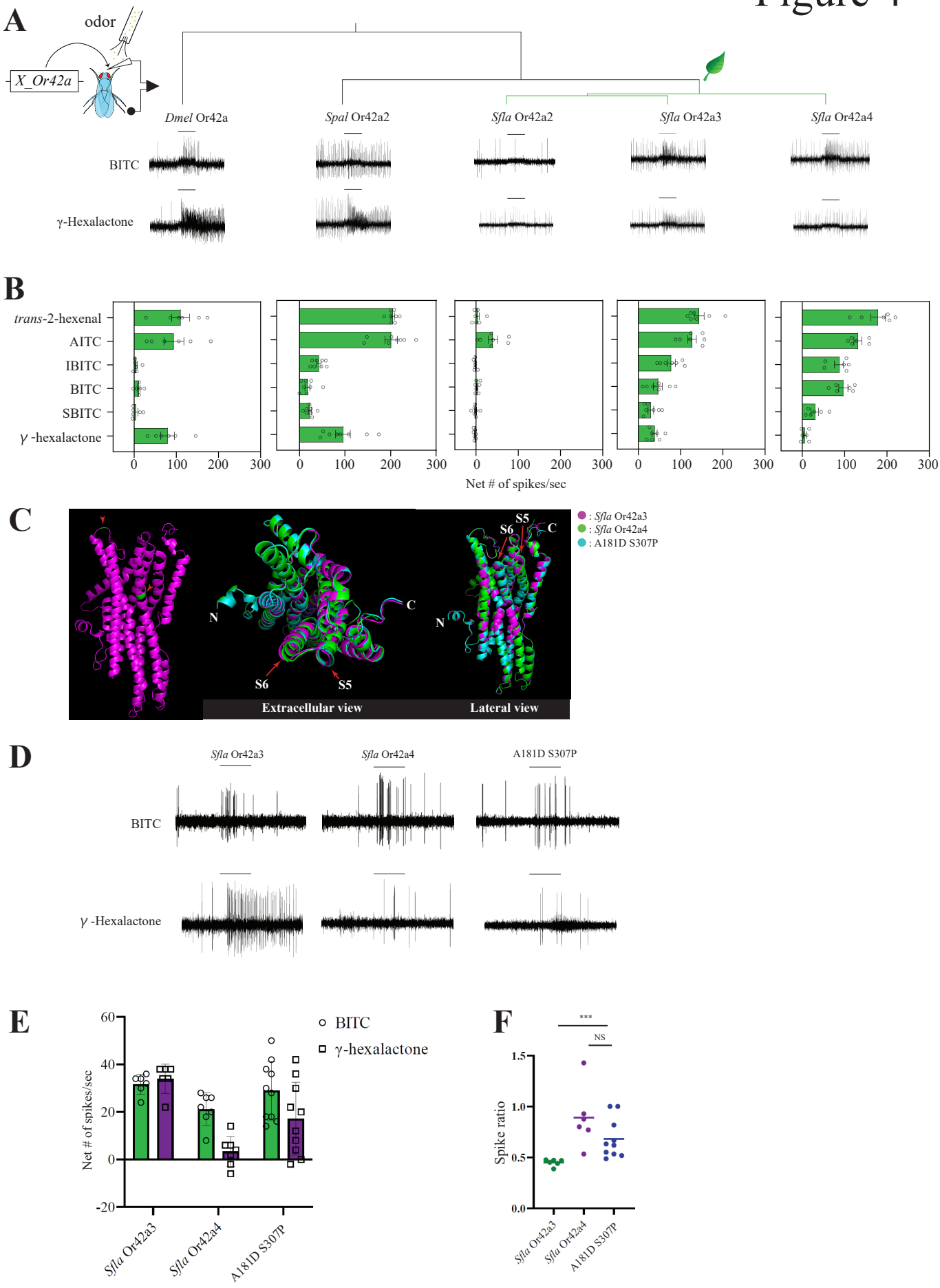
A
odor
X_Or42a
Dmel Or42a
Spal Or42a2
Sfla Or42a2
Sfla Or42a3
Sfla Or42a4
BITC
γ-Hexalactone
B
trans-2-hexenal
AITC
IBITC
BITC
SBITC
γ -hexalactone
0
100
200
300
Net # of spikes/sec
C
: Sfla Or42a3
: Sfla Or42a4
: A181D S307P
N
C
S6
S5
Extracellular view
Lateral view
D
Sfla Or42a3
Sfla Or42a4
A181D S307P
BITC
γ -Hexalactone
E
60
40
20
0
-20
Net # of spikes/sec
BITC
γ-hexalactone
Sfla Or42a3
Sfla Or42a4
A181D S307P
F
***
NS
1.5
1.0
0.5
0.0
Spike ratio
Sfla Or42a3
Sfla Or42a4
A181D S307P

Figure 1

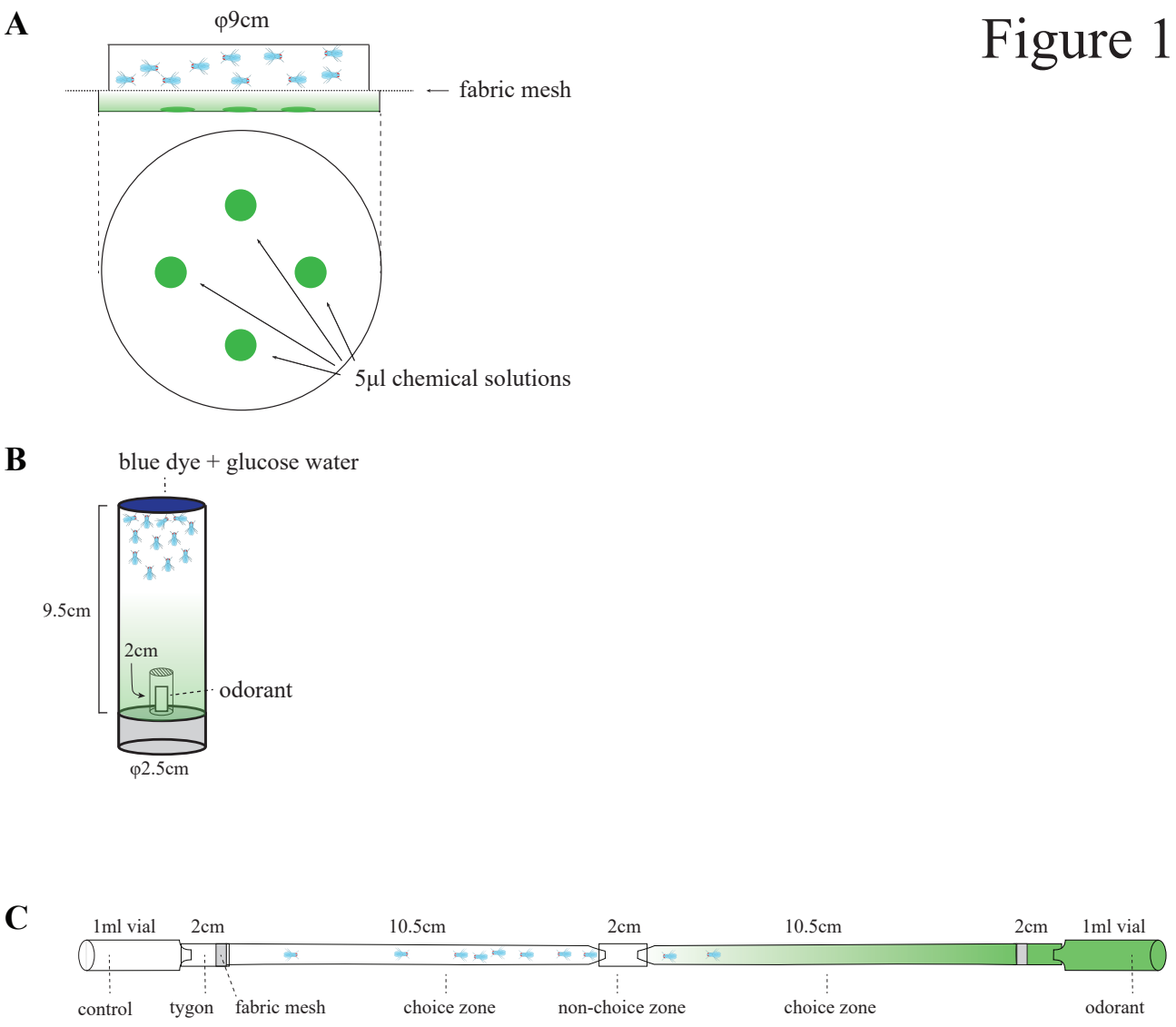
A
φ9cm
fabric mesh
5μl chemical solutions
B
blue dye + glucose water
9.5cm
2cm
odorant
φ2.5cm
C
1ml vial
2cm
10.5cm
2cm
10.5cm
2cm
1ml vial
control
tygon
fabric mesh
choice zone
non-choice zone
choice zone
odorant

Figure 2

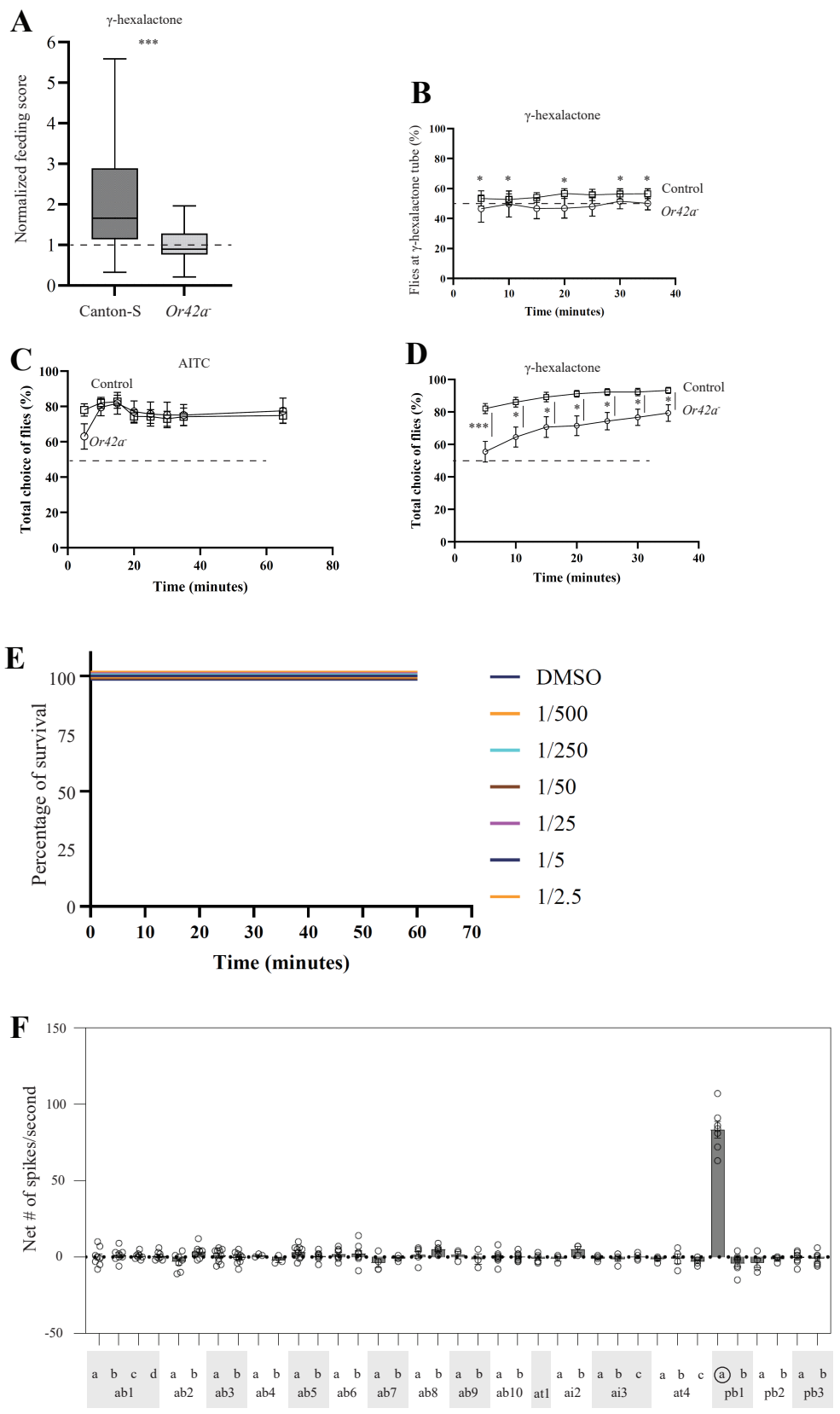
A
γ-hexalactone
***
Normalized feeding score
Canton-S
Or42a-
B
γ-hexalactone
Flies at γ-hexalactone tube (%)
Control
Or42a-
Time (minutes)
C
AITC
Control
Or42a-
Total choice of flies (%)
Time (minutes)
D
γ-hexalactone
Control
Or42a-
Total choice of flies (%)
Time (minutes)
E
Percentage of survival
Time (minutes)
DMSO
1/500
1/250
1/50
1/25
1/5
1/2.5
F
Net # of spikes/second
ab1
ab2
ab3
ab4
ab5
ab6
ab7
ab8
ab9
ab10
at1
ai2
ai3
at4
pb1
pb2
pb3

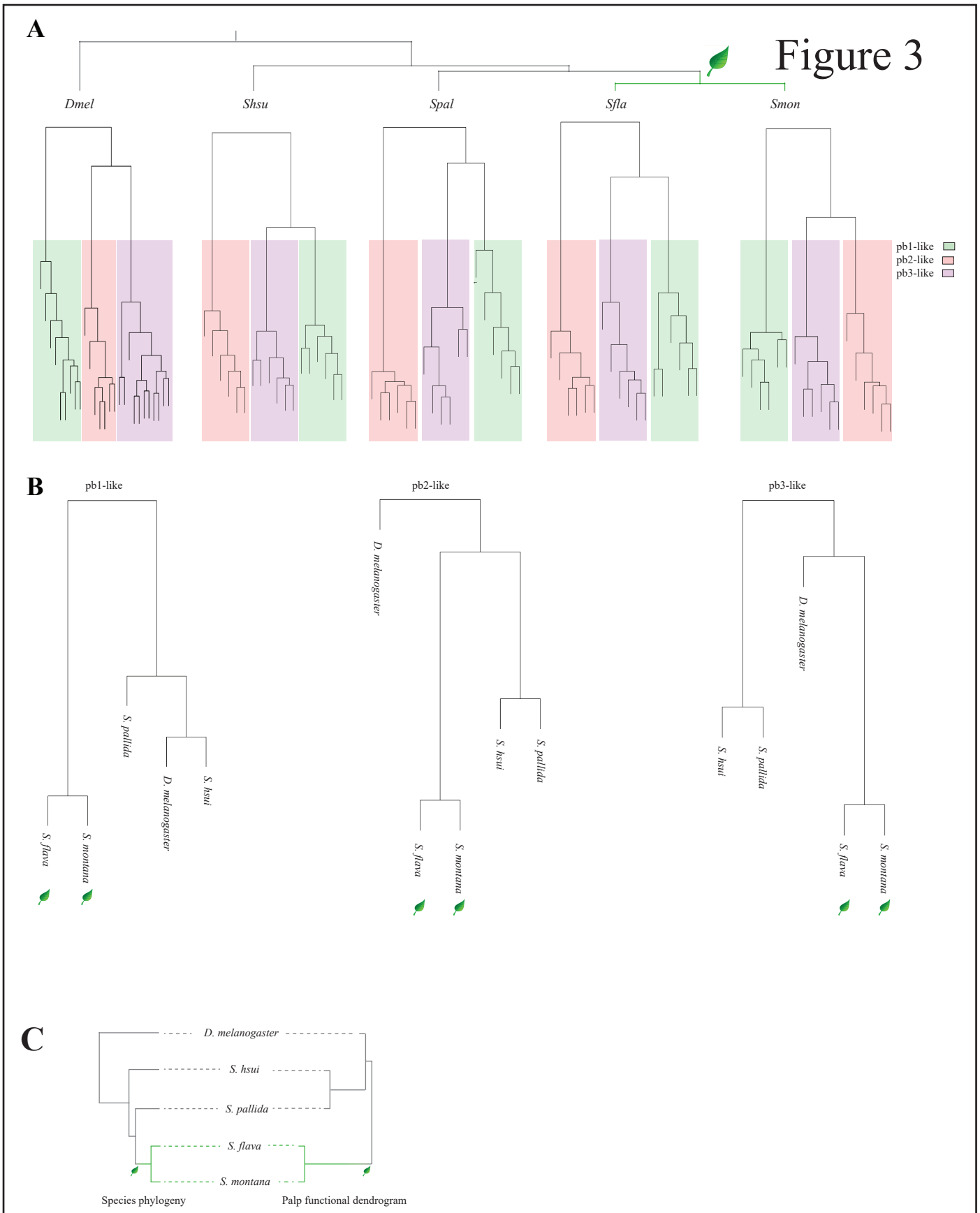
Figure 3
A
Dmel
Shsu
Spal
Sfla
Smon
pb1-like
pb2-like
pb3-like
B
pb1-like
S. flava
S. montana
D. melanogaster
S. pallida
S. hsui
pb2-like
D. melanogaster
S. flava
S. montana
S. hsui
S. pallida
pb3-like
D. melanogaster
S. hsui
S. pallida
S. flava
S. montana
C
D. melanogaster
S. hsui
S. pallida
S. flava
S. montana
Species phylogeny
Palp functional dendrogram

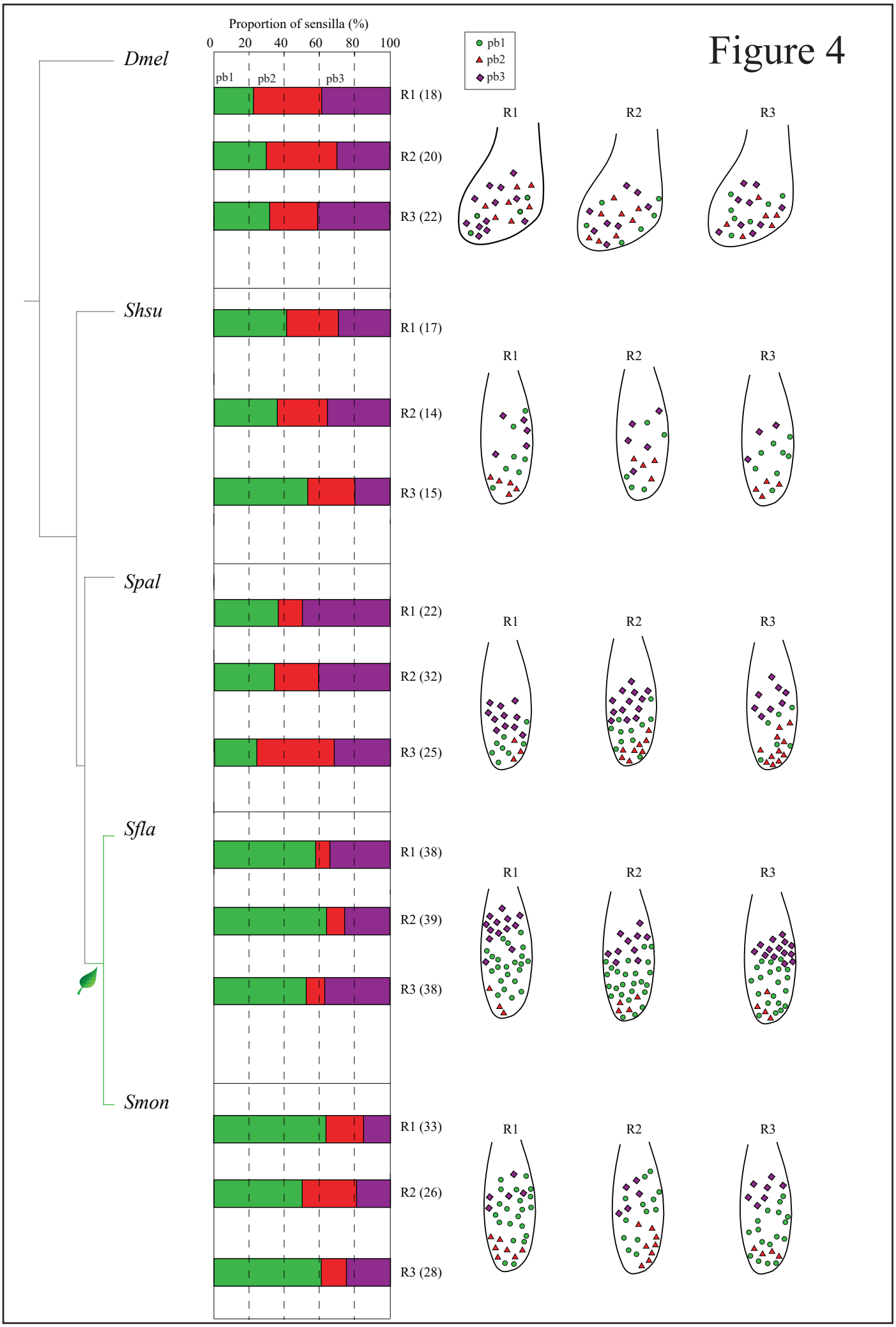
Figure 4
Proportion of sensilla (%)
0
20
40
60
80
100
pb1
pb2
pb3
Dmel
R1 (18)
R2 (20)
R3 (22)
Shsu
R1 (17)
R2 (14)
R3 (15)
Spal
R1 (22)
R2 (32)
R3 (25)
Sfla
R1 (38)
R2 (39)
R3 (38)
Smon
R1 (33)
R2 (26)
R3 (28)
R1
R2
R3

Figure 5

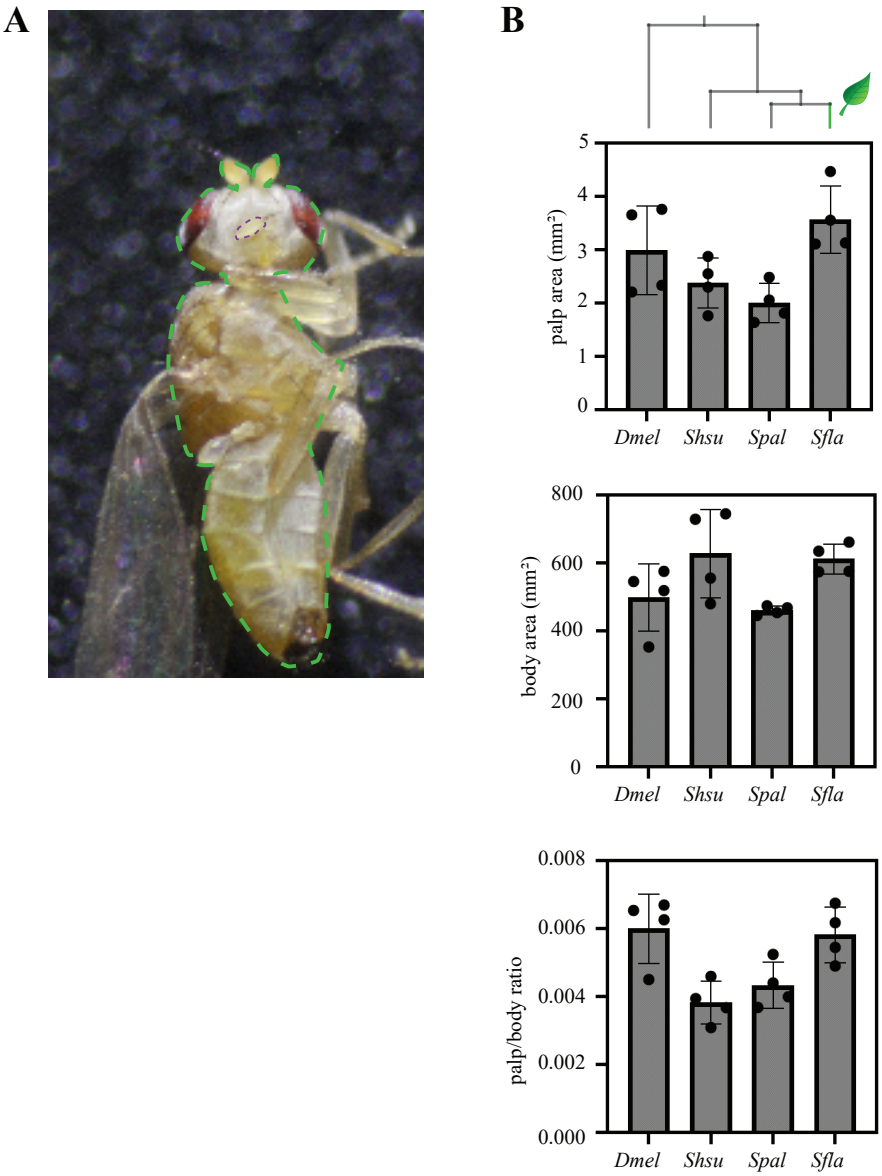
A
B
palp area (mm²)
0
1
2
3
4
5
Dmel
Shsu
Spal
Sfla
body area (mm²)
0
200
400
600
800
Dmel
Shsu
Spal
Sfla
palp/body ratio
0.000
0.002
0.004
0.006
0.008
Dmel
Shsu
Spal
Sfla

Figure 6

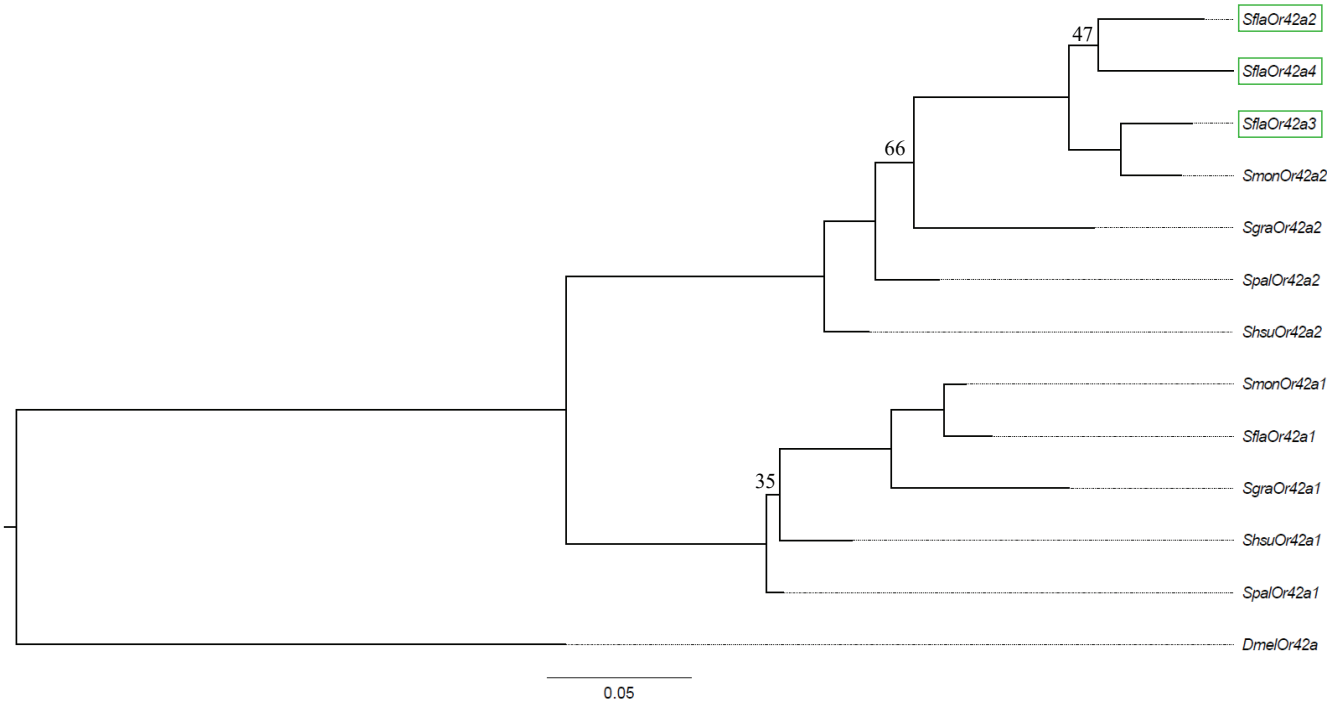
SflaOr42a2
SflaOr42a4
SflaOr42a3
SmonOr42a2
SgraOr42a2
SpalOr42a2
ShsuOr42a2
SmonOr42a1
SflaOr42a1
SgraOr42a1
ShsuOr42a1
SpalOr42a1
DmelOr42a
47
66
35
0.05

Figure 7

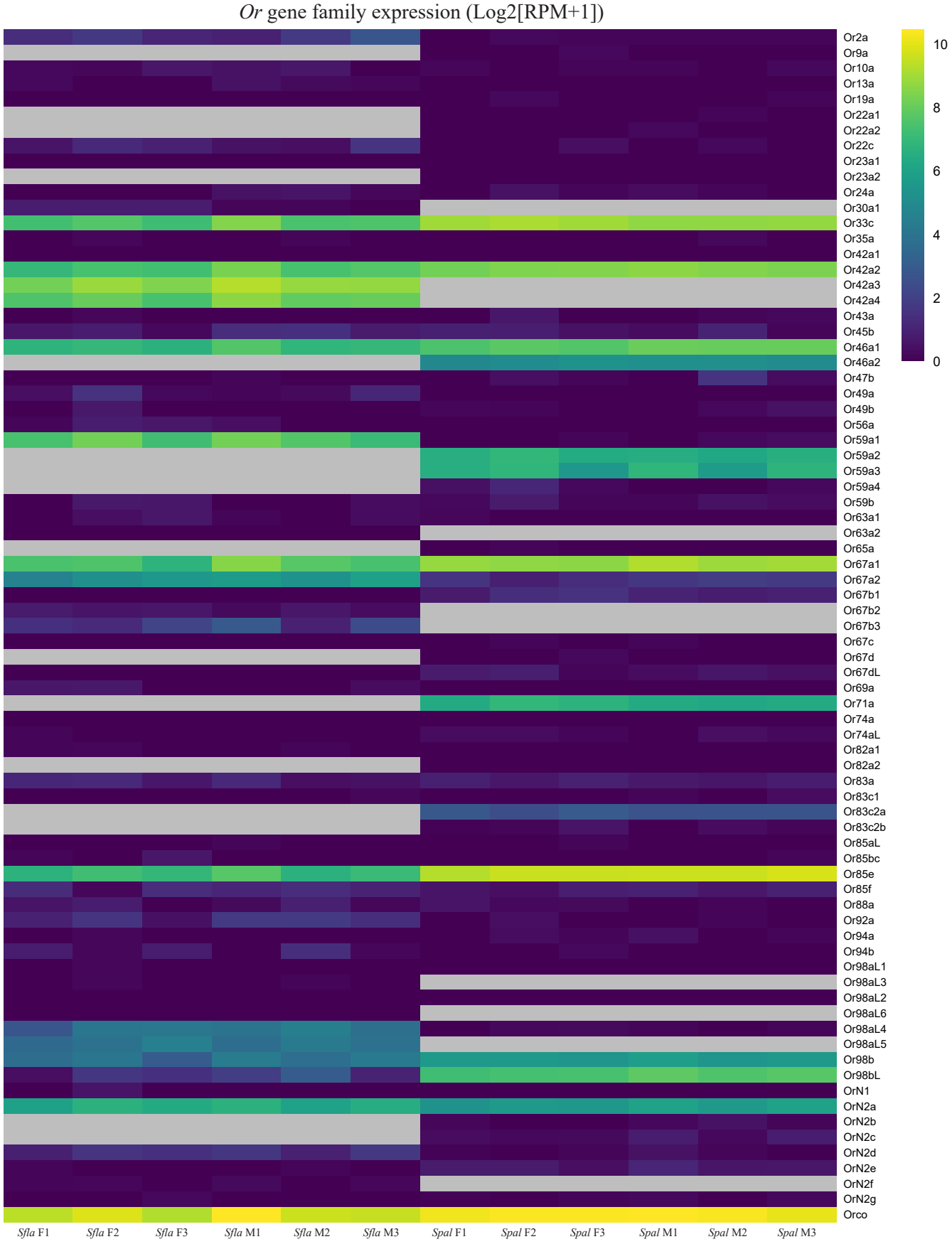
Or gene family expression (Log2[RPM+1])
Or2a
Or9a
Or10a
Or13a
Or19a
Or22a1
Or22a2
Or22c
Or23a1
Or23a2
Or24a
Or30a1
Or33c
Or35a
Or42a1
Or42a2
Or42a3
Or42a4
Or43a
Or45b
Or46a1
Or46a2
Or47b
Or49a
Or49b
Or56a
Or59a1
Or59a2
Or59a3
Or59a4
Or59b
Or63a1
Or63a2
Or65a
Or67a1
Or67a2
Or67b1
Or67b2
Or67b3
Or67c
Or67d
Or67dL
Or69a
Or71a
Or74a
Or74aL
Or82a1
Or82a2
Or83a
Or83c1
Or83c2a
Or83c2b
Or85aL
Or85bc
Or85e
Or85f
Or88a
Or92a
Or94a
Or94b
Or98aL1
Or98aL3
Or98aL2
Or98aL6
Or98aL4
Or98aL5
Or98b
Or98bL
OrN1
OrN2a
OrN2b
OrN2c
OrN2d
OrN2e
OrN2f
OrN2g
Orco
10
8
6
4
2
0
Sfla F1
Sfla F2
Sfla F3
Sfla M1
Sfla M2
Sfla M3
Spal F1
Spal F2
Spal F3
Spal M1
Spal M2
Spal M3

Figure 8

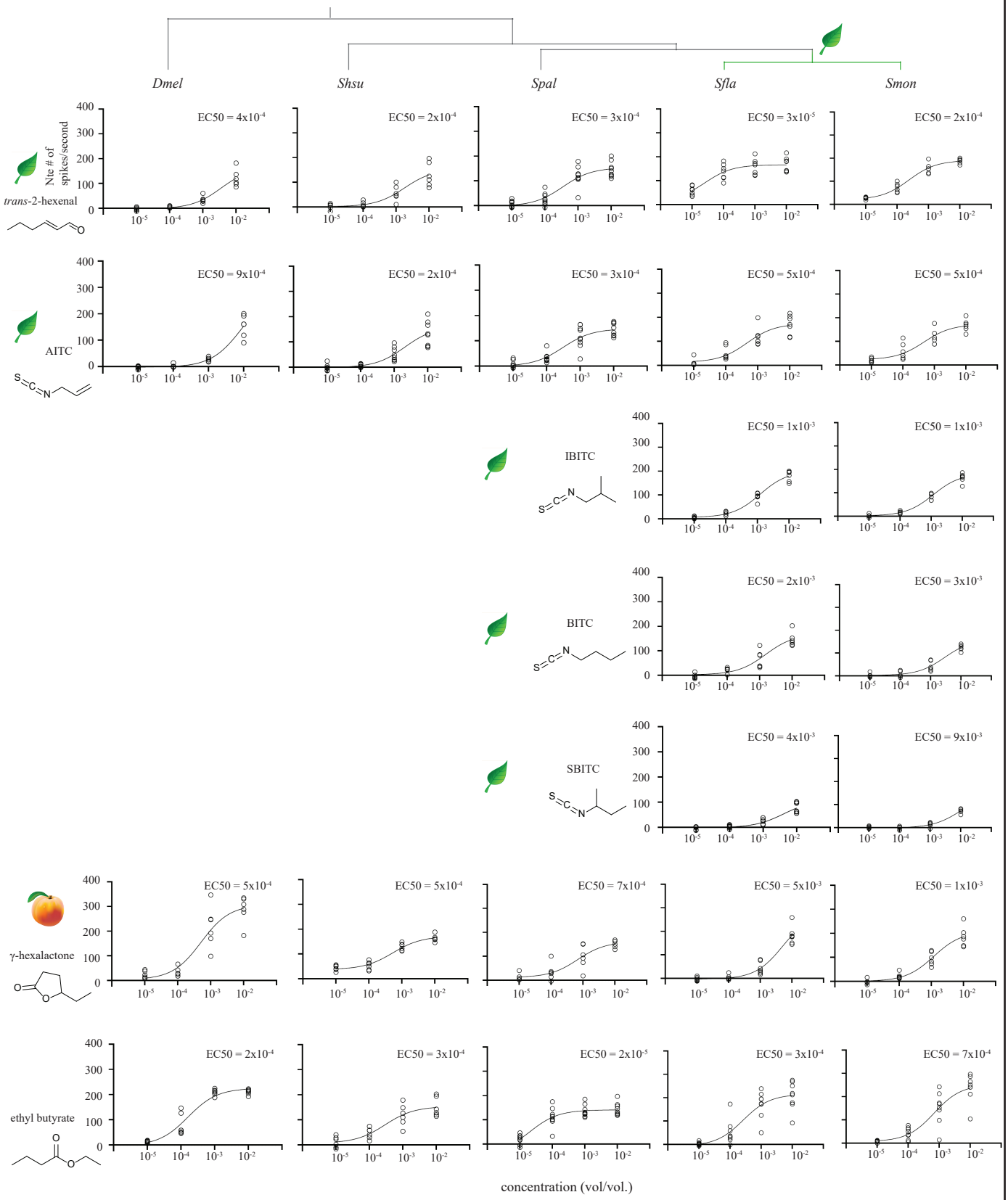
Dmel
Shsu
Spal
Sfla
Smon
Nte # of spikes/second
trans-2-hexenal
EC50 = 4x10-4
EC50 = 2x10-4
EC50 = 3x10-4
EC50 = 3x10-5
EC50 = 2x10-4
AITC
EC50 = 9x10-4
EC50 = 2x10-4
EC50 = 3x10-4
EC50 = 5x10-4
EC50 = 5x10-4
IBITC
EC50 = 1x10-3
EC50 = 1x10-3
BITC
EC50 = 2x10-3
EC50 = 3x10-3
SBITC
EC50 = 4x10-3
EC50 = 9x10-3
γ-hexalactone
EC50 = 5x10-4
EC50 = 5x10-4
EC50 = 7x10-4
EC50 = 5x10-3
EC50 = 1x10-3
ethyl butyrate
EC50 = 2x10-4
EC50 = 3x10-4
EC50 = 2x10-5
EC50 = 3x10-4
EC50 = 7x10-4
concentration (vol/vol.)

A

```
                1         10        20        30        40        50        60        70
Consensus       MVLRNIFPSLYAKPDSAPPESRKATLYLLRCVFLMGIRTPPQRYFLIYCLWSFALNXSSTFYQPIGFMLXYISHL
Spal Or42a2     MVLRKIFPSMYAKPDSAPPESRKATLYLLRCVFLMGIRTPPQRFFLIYCLWSFALNLSSTFYQPIGFMTGYISHL
Sfla Or42a3     MVLRNIFPSLYAKPDSAPPESRKATLYLLRCVFLMGIRTPPQRYFLIYCLWSFALNMSSTFYQPIGFMLAYISHL
Sfla Or42a4     MVLRNIFPSLYAKPDSAPPESRKATLYLLRCVFLMGIRTPPQRYFLIYCLWSFALNLSSTFYQPIGFLMGYISHL
A181D, S301P    MVLRNIFPSLYAKPDSAPPESRKATLYLLRCVFLMGIRTPPQRYFLIYCLWSFALNMSSTFYQPIGFMLAYISHL

                80        90        100       110       120       130       140       150
Consensus       SELSPGEFLTSLQVAFNXWACSTKVIIVWVLXKRFDZANLLLDKLDXXLKKPSXRARSHRAVANSNRXFFCFMTV
Spal Or42a2     SEFSPGEFLTSLQVAFNAWSCSTKVIIVWVLVNRFDQANRILDKLDERLTKPSERARSHRAVASSNRIFFCFMTV
Sfla Or42a3     SELSPGEFLTSLQVAFNTWACSTKVIIVWVLAKRFDEANLLLDKLDKQLKKPSDRARSHRAVANSNRFFFCFMTV
Sfla Or42a4     SELSPGELLTSLQVAFNAWACSTKVIIVWVQVKRFDQANLLLDKLDERLKKPSERARSHRAVANSNRIYFCFMTV
A181D, S301P    SELSPGEFLTSLQVAFNTWACSTKVIIVWVLAKRFDEANLLLDKLDKQLKKPSDRARSHRAVANSNRFFFCFMTV

                160       170       180       190       200       210       220
Consensus       XVLYATSXAVSAAAMGVPSFQNYYPWLDWRXSKWQFWLQSGLEYFAMLGACFQDACLDCFPINFVVPLRAHVANL
Spal Or42a2     YLLYATSTAVSAAAMGVPSFQNYYPWLDWRASKWQFWLQSGLEYFAMLGACFQDVCVDCYPINFVLPLRAHMANF
Sfla Or42a3     NVLYATSAAVSAAAMGVPSFQNYYPWLDWRASKWQFWLQSGLEYFAMLGACFQDACLDCFPINFVVPLRAHVANL
Sfla Or42a4     YILYATSTAVSAAVMGVPSFQNYYPWLDWRDSKWQFWLQSGLEYFAMLGACFQDACLDCFPINFVVPLRAHIANL
A181D, S301P    NVLYATSAAVSAAAMGVPSFQNYYPWLDWRDSKWQFWLQSGLEYFAMLGACFQDACLDCFPINFVVPLRAHVANL

                230       240       250       260       270       280       290       300
Consensus       ADRLRQLGNNPEEQPEQRYEKLIECIQDHKVILSFCDTLRPIIGGTIFVQLLVVGLLLGFTIINIVMFANFXSRI
Spal Or42a2     ADRLRQLGNNPDEQPEQRYEKLIECIHDHKVILSFCDTLRPMIGGTIFVQLLVVGLVLGFTIINIVMFANFGSRI
Sfla Or42a3     ADRLRQLGNNPEEQPEQRYEKLIECIQDHKVILSFCDTLRPIIGGTIFVQLLVVGLLLGFTIINIVMFANFASRI
Sfla Or42a4     AERLRELGNNPEEQPEQRYEKLIECIQDHKVILSFCDILRPIIGGTIFVQLLIVGLILGFTIINIVVFANFGSRI
A181D, S301P    ADRLRQLGNNPEEQPEQRYEKLIECIQDHKVILSFCDTLRPIIGGTIFVQLLVVGLLLGFTIINIVMFANFASRI

                310       320       330*      340       350       360       370
Consensus       AAMSYMXAVLLETTPFCILCNYLADDCNKLADALFESNWIDQEQRYKKTVLQFLQSLQKPIVFMAGNLFEISVAT
Spal Or42a2     AAMSFMSAVLLETTPFCILCNYLADDCSKLADALFESNWIDQEQRYKKTLLQFLQSLQKPIVFTAGNILTISVAT
Sfla Or42a3     AAMSYMSAVLLETTPFCILCNYLADDCNKLADALFESNWIDQEQRYKKTVLQFLQSLQKPIVFMAGNLFEISVAT
Sfla Or42a4     AAISYVPAVLLETTPFCILCNYLADDCNKLSDALFESNWIDQEQRYKKTVLQFLQSLQKPIVFMAGNLFEISVAT
A181D, S301P    AAMSYMPAVLLETTPFCILCNYLADDCNKLADALFESNWIDQEQRYKKTVLQFLQSLQKPIVFMAGNLFEISVAT

                380       *390      400       407
Consensus       NLNATKFSFTVFTLVKQMNIAEKLSKPSELIL
Spal Or42a2     NLNATKFSFSVFTLVKQMNIAEKLSKPSETE
Sfla Or42a3     NLNATKFSFTVFTLVKQMNIAEKLSKPSELIL
Sfla Or42a4     NLNATKFSFTVFTFVKQMNIAEKLSKPSE
A181D, S301P    NLNATKFSFTVFTLVKQMNIAEKLSKPSELIL
```

B

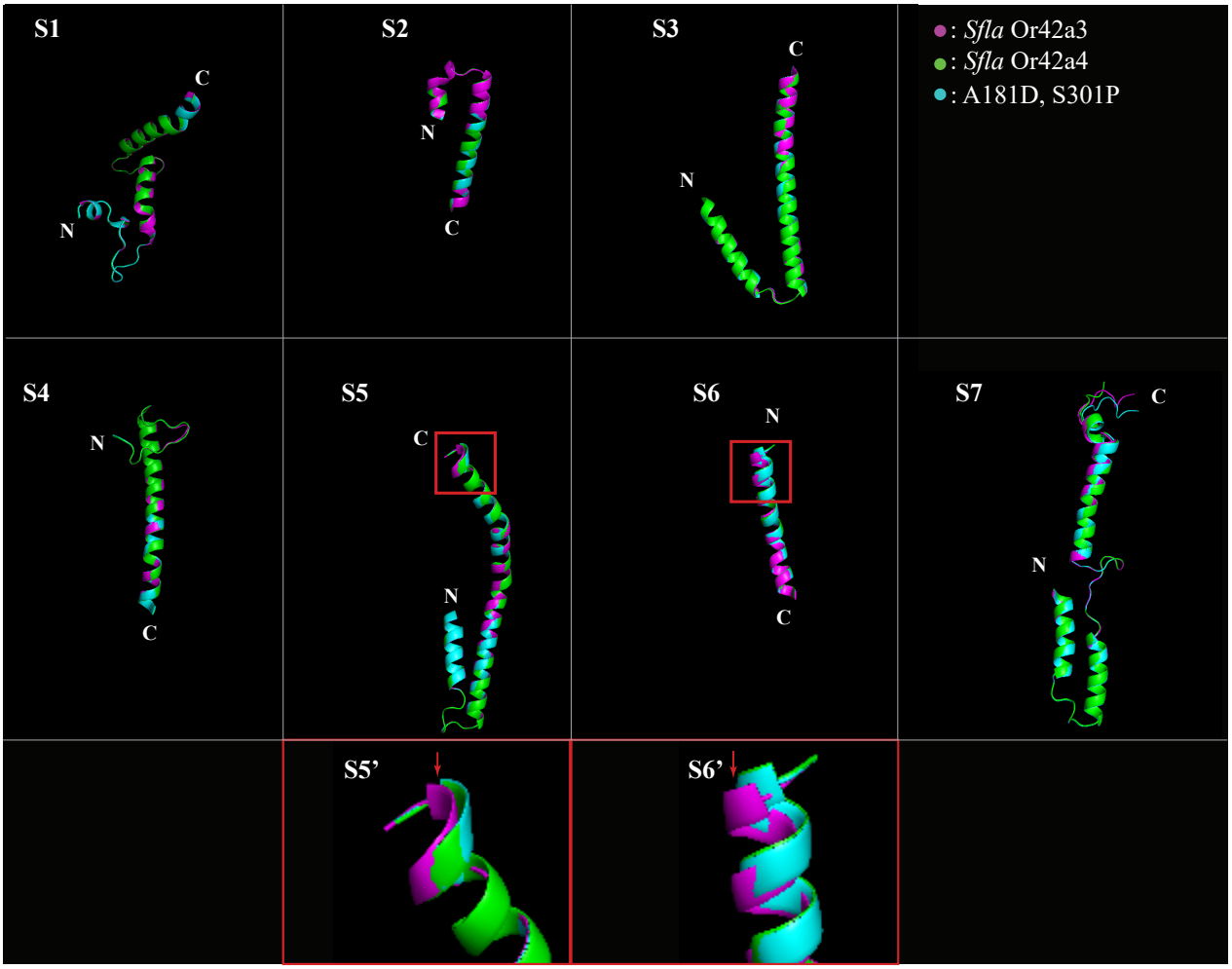

Figure 10

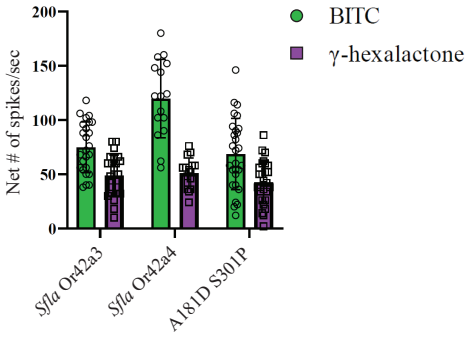
BITC
γ-hexalactone
Net # of spikes/sec
200
150
100
50
0
Sfla Or42a3
Sfla Or42a4
A181D S301P

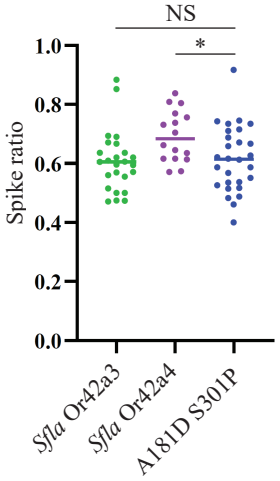
NS
*
Spike ratio
1.0
0.8
0.6
0.4
0.2
0.0
Sfla Or42a3
Sfla Or42a4
A181D S301P